Accepted Manuscript

Design, synthesis and identification of novel substituted 2-amino thiazole analogues as potential anti-inflammatory agents targeting 5-lipoxygenase

Shweta Sinha, Mukesh Doble, S.L. Manju

PII: S0223-5234(18)30770-0

DOI: 10.1016/j.ejmech.2018.08.098

Reference: EJMECH 10709

To appear in: *European Journal of Medicinal Chemistry*

Received Date: 25 December 2017

Revised Date: 28 August 2018

Accepted Date: 31 August 2018

Please cite this article as: S. Sinha, M. Doble, S.L. Manju, Design, synthesis and identification of novel substituted 2-amino thiazole analogues as potential anti-inflammatory agents targeting 5-lipoxygenase, *European Journal of Medicinal Chemistry* (2018), doi: 10.1016/j.ejmech.2018.08.098.

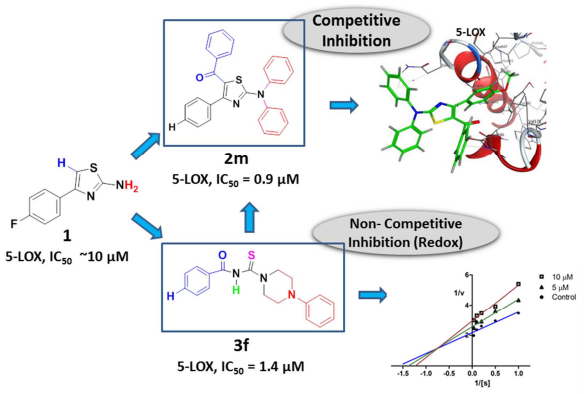

Design, synthesis and identification of novel substituted 2-amino thiazole analogues as potential anti-inflammatory agents targeting 5-Lipoxygenase

Shweta Sinha[a,b], Mukesh Doble[b,]*, S. L Manju[a,]*

[a]*Department of Chemistry, Vellore Institute of Technology, Vellore, Tamil Nadu, 632014, India.*
[b]*Department of Biotechnology, Indian Institute of Technology, Madras, Tamil Nadu, 600036, India.*

**Corresponding authors*
Email: mukeshd@iitm.ac.in, slmanju@vit.ac.in

***Keywords*:** Design, Inflammation, 5-Lipoxygenase**,** Pharmacophore/Docking, Thiazoles.

Highlights

- Novel thiazoles/thioureas are designed via pharmacophore modeling against 5-LOX.
- Most compounds found active against 5-LOX *in vitro* enzyme inhibition studies.
- The best compound, 2**m,** from thiazole series acts as a competitive 5-LOX inhibitor.
- The most potent thiourea, **3f,** inhibits 5-LOX via non-competitive (redox) mechanism.
- Docking studies demonstrate binding mode of the competitive inhibitors.

ABSRACT

Human 5-Lipoxygenase (5-LOX) is a key enzyme targeted for asthma and inflammation. Zileuton, the only drug against 5-LOX, was withdrawn from the market due to several problems. In the present study, the performance of rationally designed conjugates of thiazole (**2**) and thiourea (**3**) scaffolds from our previously reported 2-amino-4-aryl thiazole **(1)** is reported. They are synthesized (total 31 derivatives), characterized, and tested against the 5-LOX enzyme *in vitro* and the mode of action of the most active ones are determined. Compound **2m** exhibited an IC_{50} of 0.9 ± 0.1 µM acting through competitive (non-redox) mechanism, unlike Zileuton, and found to be devoid of radical scavenging properties. Computational studies are in good agreement with the experimental data supporting its mechanism of action. Another lead molecule from the thiourea series (**3**), **3f,** exhibited an IC_{50} of 1.4 ± 0.1 µM against 5-LOX whose mode of action is redox type (non-competitive). It is promising to note that the activities displayed by both the lead inhibitors, **2m** and **3f,** are better than the commercial drug, Zileuton (IC_{50} = 1.5 ± 0.3 µM). These inhibitors could be further developed as drugs against inflammation.

1. Introduction

Chronic inflammation is implicated in a variety of diseases including asthma, allergy, arthritis, cancer, cardiovascular and respiratory tract disorders [1-3]. These inflammatory diseases are directly or indirectly related with the alterations in the production of leukotrienes (LTs) and prostaglandins (PGs) in the arachidonic acid (AA) pathway [4,5]. Several studies have demonstrated that 5-lipoxygenase (5-LOX) is an important enzyme which catalyzes AA for the production of several LTs. It oxygenates AA into 5(S)-hydroperoxyeicosatetraenoic acid (5-HPETE) and further dehydrates to leukotriene A4 (LTA4) [6,7] Therefore, 5-LOX is regarded as a valid target against inflammation in the drug discovery. In the past several years, different classes of low molecular weight 5-LOX inhibitors (i.e. redox, non-redox and iron chelator) have been developed [8]. Inhibitors including benzoquinones [9], benzimidazoles [10] and triazole caffeic acid esters [11] have been shown to inhibit this enzyme effectively. The only 5-LOX inhibitor which could enter the market as an anti-inflammatory drug for the treatment of asthma was, Zileuton, with an IC_{50} ~1 μM [12] But its use is restricted, due to drawbacks of liver toxicity and short half-life, [13] thereby, creating a dire need for the design and development of new chemical entities against inflammation.

Pharmacophore modeling is one of the widely used strategies in the ligand-based drug design. Pharmacophore is a set of features comprising of H-bond donor, H-bond acceptor, hydrophobic centroid and aromatic center, essential for the enzyme-ligand interaction in the active molecule [14]. Thiazole is a unique heterocycle containing sulphur and nitrogen atoms and is considered as a building block of many drug candidates in medicinal chemistry. They are known to have antimicrobial, anticancer, anti-inflammatory and anti-HIV properties [15-17]. Previous reports have shown that N,4-diaryl-1,3-thiazole-2-amine derivatives containing thiazole as the basic

moiety are selective inhibitors of 5-LOX and COX-2 [18]. A series of 4-monosubstituted 2-aminothiazole pirinixic acid derivatives bearing thiazole as core molecule have been reported as dual 5-LOX and mPGES1 inhibitors [19]. Recently, 2-amino-4-aryl thiazoles (**1**) have been identified by us as a potent competitive type of 5-LOX inhibitors [20]. In continuation of our earlier work, a series of novel (4-(4-substituted phenyl)-2-(substituted amino-1-yl)thiazol-5-yl)(phenyl)methanone derivatives (**2**) have been designed and synthesized by us with better efficacy and potency (Figure 1). With an aim to increase the potency of basic thiazole pharmacophore, hydrophobic centroids and H-bond acceptor features were introduced in the molecule (**2**) by incorporating benzoyl group at the 5^{th} and substituted secondary (2^0) amine at the 2^{nd} positions in the thiazole ring. Different aryl substitutions at the 4^{th} position of the thiazole ring are incorporated to investigate the effect of benzoyl and 2^0 amine substituents on the potency against 5-LOX enzyme.

The known drug, Zileuton (N-(1-benzo[b]thien-2-ylethyl)-N-hydroxyurea) and a compound in clinical trial, MLN977 (1-(4-(5-((4-fluorophenoxy)methyl)tetrahydrofuran-2-yl)but-3-ynyl)-1-hydroxyurea) from N-hydroxyurea series have N-hydroxyurea group in common. MLN977 has also been discontinued in Phase II clinical trials due to side effect, namely elevations in liver enzyme [21]. Perhaps, N-hydroxyurea group is acting through free radical-mediated lipid peroxidation of cell membrane and possibly responsible for the hepatotoxicity [22,23]. Based on these facts as well as to achieve improved safety profile of the drug candidate, the scaffold has been modified by replacing the urea with a thiourea group as the basic moiety and the designed another series of novel compounds (**3)**. Further structural modifications are carried out by substituting both the nitrogens of the thiourea. The first nitrogen is substituted with a secondary amine and the other with a substituted benzoyl group at N-H position in (**3**) (Fig. 1).

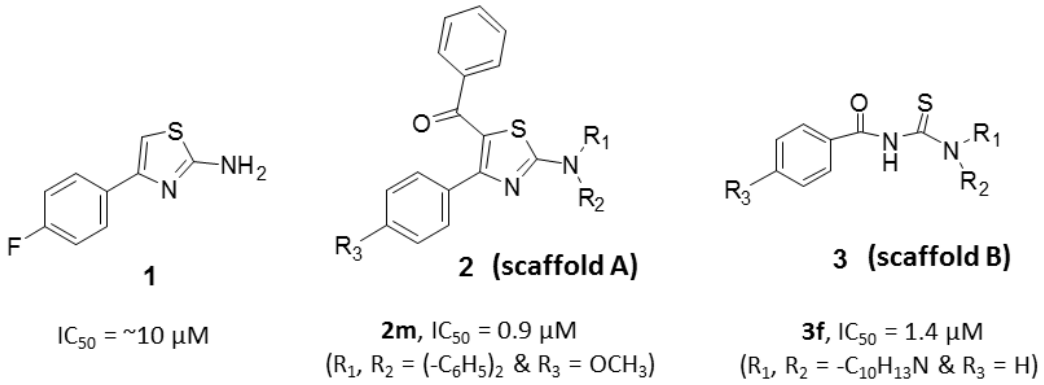

Fig. 1: General structures of novel scaffolds A (**2**) and B **(3**) including (**1**) previously reported compound considered as the starting scaffold for the design of molecule **2**.

This paper discusses the ligand based drug design strategy including pharmacophore modeling and then synthesis of a series of (4-(4-substituted phenyl)-2-(amino-1-yl)thiazol-5-yl)(phenyl)methanone (**2**) and 4-substituted-N-(amino-1-carbonothioyl)benzamide (**3**) scaffolds. *In vitro* 5-LOX inhibitory activity as well as their mechanism of action of these synthesized compounds is also studied.

2. Results and discussion

2.1. Design

Thiazole is a vital core scaffold present in several medicinally significant natural and synthetic compounds. Previous studies indicate that 2-amino-4-aryl thiazole is an effective 5-LOX inhibitor, among which compound **1** exhibits the highest activity with an IC_{50} of ~10 µM [20]. To further improve the potency and bring down the IC_{50} value of molecule **1**, hydrophobic centroids and H-bond acceptor features are introduced (Fig. 2). The reason for introducing these features are based on pharmacophore studies as described below.

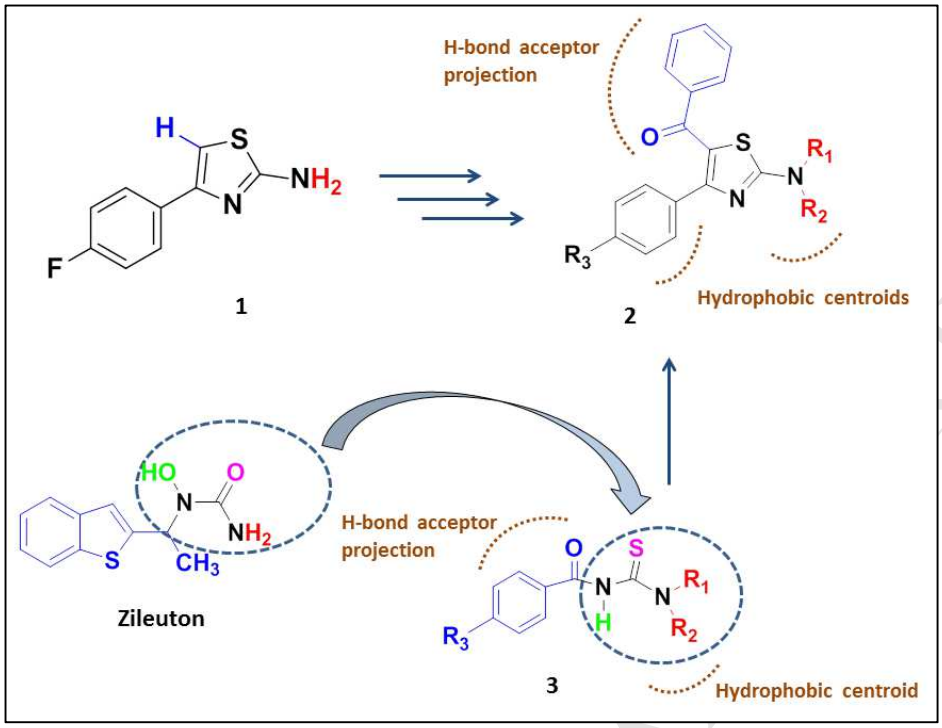

Fig. 2: Design of novel compound (4-(4-substituted phenyl)-2-(amino-1-yl)thiazol-5-yl)(phenyl)methanone (**2**) and 4-substituted-N-(amino-1-carbonothioyl)benzamide (**3**) from **1** and Zileuton respectively.

2.2. Pharmacophore elucidation

A pharmacophore is a set of essential features used to correlate the biological activities for a group of compounds with their chemical structures [24, 25]. To determine the features essential for 5-LOX inhibition, a pharmacophore model was developed from the group of known 5-LOX inhibitors reported in the literature, namely, Zileuton, Atrleuton, MLN977, Licofelone, Siteleuton, and PF4191834 (Fig. 3).

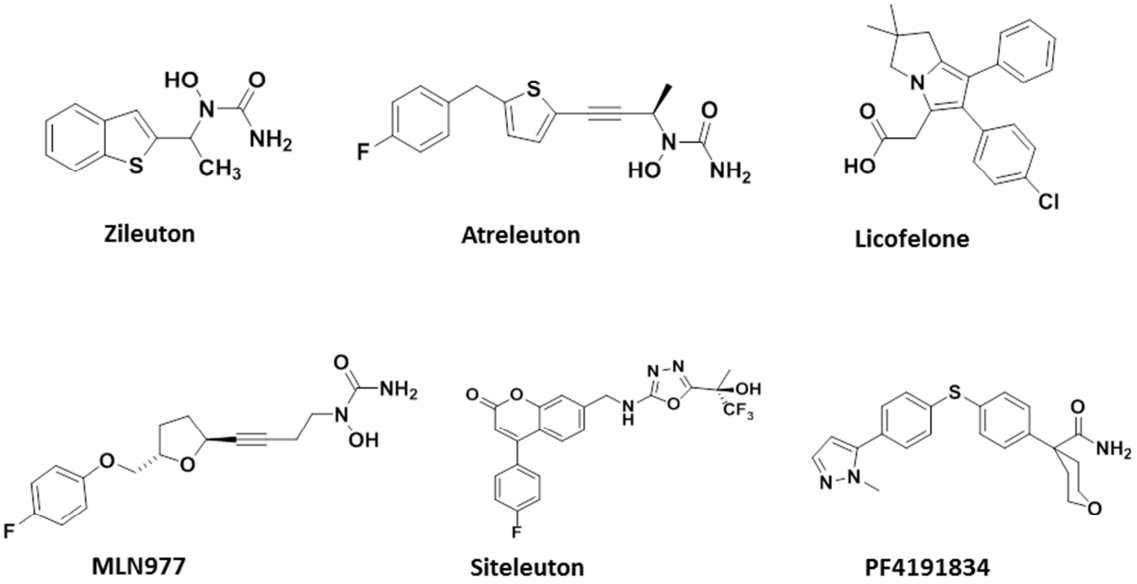

Fig. 3: Structures of known 5-LOX inhibitors.

Zileuton is a well-known drug from N-hydroxy urea series available for asthma with restrictions. Atrleuton and MLN977 are under phase II clinical trials. The latter has been discontinued due to liver enzyme elevations. All these three inhibitors have a common group, namely N-hydroxy urea. Licofelone is a multi-targeted inhibitor for FLAP, mPGES1 and 5-LOX with a pyrrolizine ring. Siteleuton is a coumarin derivative under clinical trials and is terminated due to liver toxicity. PF4191834, with a pyrazole moeity is a selective 5-LOX inhibitor under clinical trial and is effective for pain and inflammation [26,27]. These six inhibitors have a four-point pharmacophoric features (Ph model) containing two hydrophobic centroids (Hyd) and two H-bond acceptors (Acc2) (Figure 4a). Hence, compound **2** is designed by introducing a hydrophobic centroid and H-bond acceptor in compound **1,** namely a benzoyl group is inserted at the 5^{th} position and substituted secondary (2^0) amine at the 2^{nd} position in the thiazole ring. Compound, **3,** is designed by incorporating a benzoyl group (H-bond acceptor) at the N-H position in the thiourea moiety (Fig. 2).

An in-house conformational database of the designed compounds (listed in Table 1 and 2) are created and set as a query against Ph model. It is found that all the features of Ph model are mapped with the best molecule **2m** as well as eight other compounds from the (4-(4-substituted phenyl)-2-(amino-1-yl)thiazol-5-yl)(phenyl)methanone (**2**) series. Similarly, all the four common pharmacophore features required for the 5-LOX inhibition (as per Ph model) are mapped on to **3f** as well as fourteen other compounds of the 4-substituted-N-(amino-1-carbonothioyl)benzamide (**3**) series (Fig. 4).

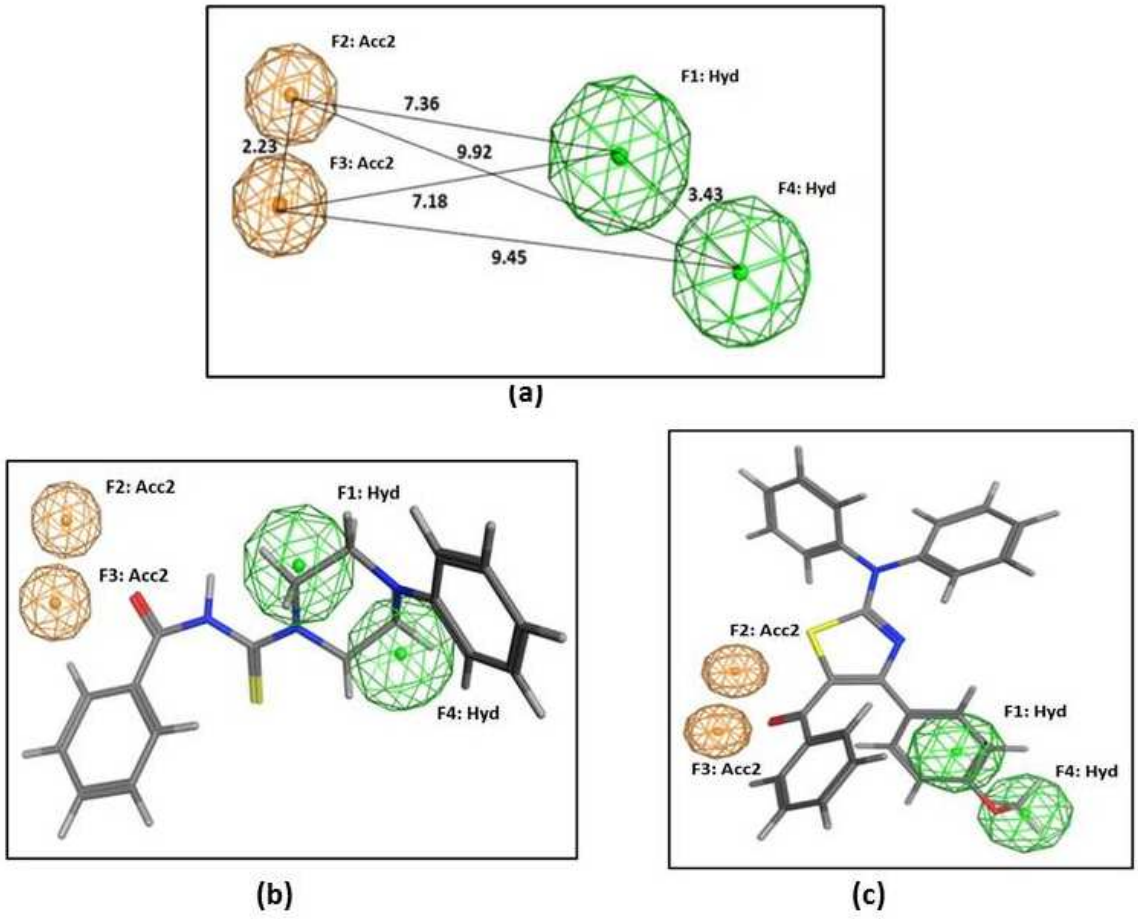

Fig. 4: a) Pharmacophore (Ph model) for 5-LOX inhibitors generated by pharmacophore elucidation in MOE 2016.0801 with 3D spatial relationship and geometric distances in A^0; b) **3f** mapping with Ph model ; c) **2m** mapping with Ph model. Pharmacophore features depicted are Hyd- Hydrophobic (green) and Acc2- H-bond acceptor (orange). Distances are given in A^0.

2.3. Chemistry

The multi-step synthesis of 4-substituted-N-(amino-1-carbonothioyl)benzamides (**3a-q**) and (4-(4-substituted phenyl)-2-(amino-1-yl)thiazol-5-yl)(phenyl)methanones (**2a-n**) is accomplished as shown in schemes 1 and 2 respectively. The intermediates (**3a-q**) and lead compounds (**2a-n**) were synthesized according to the procedure described in the literature with some modification [28,29]. The first step in the scheme 1 includes the formation of substituted benzoyl isothiocyanates. This is achieved when substituted benzoyl chloride in toluene is added to the mixture of aq. solution of potassium thiocyanate and cetrimide. This is followed by the addition of a secondary amine to the aromatic layer at 0-25 ^{0}C, stirring at room temperature for 2 h to obtain various benzamides (**3a-q**) (Scheme1).

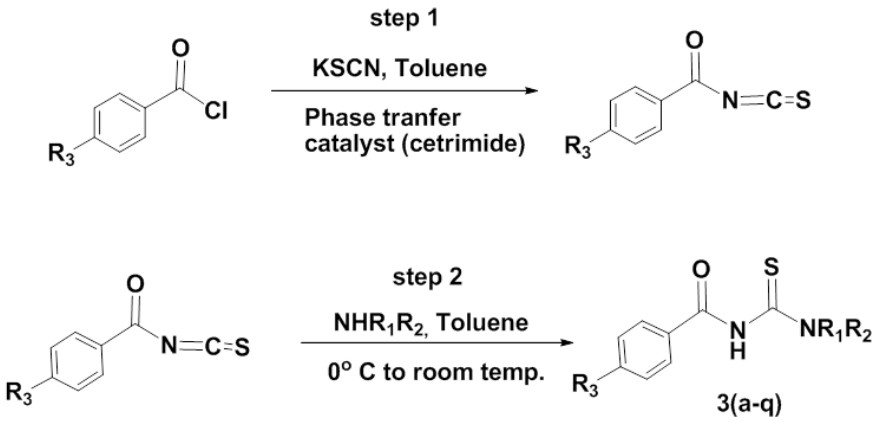

Scheme 1: Synthesis of 4-substituted-N-(amino-1-carbonothioyl)benzamide (**3a-q**) derivatives.

The synthesis of (4-(4-substituted phenyl)-2-(amino-1-yl)thiazol-5-yl)(phenyl)methanone derivatives (**2a-n**) is performed by Hantzsch thiazole synthesis procedure [28,29]. Condensation

of 2-bromoacetophenone with equivalent amount of various benzamides in the presence of catalyst, triethylamine, in acetonitrile at 70 ^{0}C results in [1+4] thiazole ring formation to give **2a-n** (Scheme 2).

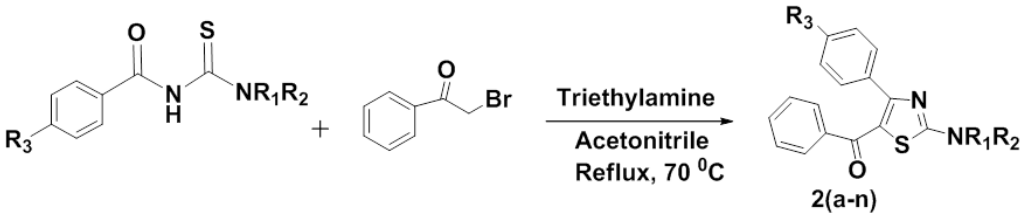

NR_1R_2 = Piperidine, Morpholine, Pyrrolidine, N-Benzylmethylamine, N-Methyl aniline, N-Phenyl Piperazine, Diphenylamine.

R_3 = H, OCH_3, F, NO_2

Scheme 2: Synthesis of (4-(4-substituted phenyl)-2-(amino-1-yl)thiazol-5-yl)(phenyl)methanone (**2a-n**) derivatives.

2.4. 5-LOX inhibitory activity

The anti-inflammatory potencies of these synthesized 2-substituted amino-4-substituted phenyl thiazol-5-yl phenyl methanones (**2a-n**) and N-(substituted carbonothioyl)-4-substituted benzamides (**3a-q**) at a concentration of 10 µM are evaluated in cell free assay using partially purified human recombinant 5-LOX enzyme (Tables 1 and 2). The activity is determined by measuring the product, 5-HPETE, produced from AA at λ_{236} [30,31]. Most of the test compounds from both the series are found to be significantly active against the enzyme 5-LOX. Zileuton is used as the positive control while DMSO (2%, v/v) as the negative control. The former inhibited 5-LOX by 86.9 ± 2.2 % (Table 1) as expected while vehicle control (2% DMSO in assay mixture

solution) did not show any inhibition. Compounds **2m** and **3f** exhibited excellent activities, almost comparable to Zileuton.

Table 1: 5-LOX inhibition and antioxidant activities of (4-(4-substituted phenyl)-2-(amino-1-yl)thiazol-5-yl)(phenyl)methanone derivatives (**2a-n**). Data are expressed as means ± SD obtained from three independent experiments.

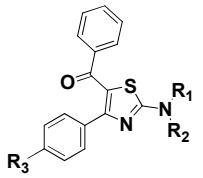

S.No.	Compd code	Structure	% 5-LOX Inhibition ± SD (10 µM)	% scavenging of DPPH ± SD (20 µM)
1	2a	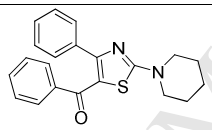	85.2 ± 8.2	8.5 ± 0.2
2	2b	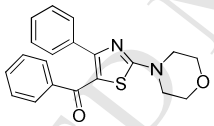	85.3 ± 6.6	9.5 ± 0.7
3	2c	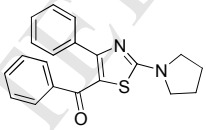	75.3 ± 3.8	-2.9 ± 0.1
4	2d	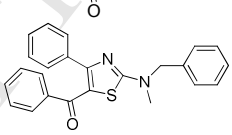	53.1 ± 1.5	3.6 ± 2.9
5	2e	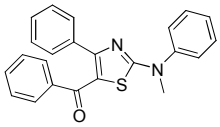	67.8 ± 2.9	4.6 ± 3.8
6	2f	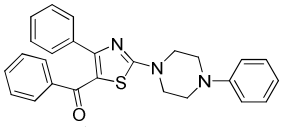	38.3 ± 2.9	-0.7 ± 1.2
7	2g	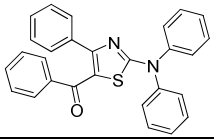	48.6 ± 0.7	-4.7 ± 0.3

8	**2h**		62.0 ± 9.4	9.6 ± 1.4
9	**2i**		17.7 ± 2.9	-1.9 ± 1.8
10	**2j**		67.8 ± 1.5	8.2 ± 4.6
11	**2k**		50.2 ± 4.4	-0.8 ± 0.4
12	**2l**		53.1 ± 2.9	7.8 ± 1.6
13	**2m**		92.8 ± 0.7	11.8 ± 2.1
14	**2n**		79.6 ± 1.5	-2.8 ± 1.0
	Zileuton		86.9 ± 2.2	17.8 ± 1.2
	Ascorbic acid	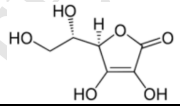	-	84.1 ± 0.5

2.5. Structure activity relationship (SAR) of 5-LOX inhibition

Analogues of **2** and **3** are synthesized to evaluate the roles of the substituents, R_1, R_2 (hydrophobic) and R_3 (H-bond acceptor) in the parent molecule for the inhibition of 5-LOX. Previous study with thiazole derivatives had indicated, that compound **1** (Fig. 1) was the most potent 5-LOX inhibitor with an IC_{50} of ~10 μM [20]. Interestingly, introducing a benzoyl residue and a 2^0amine (diphenylamine) in the central thiazole ring (**2**) yielded a highly potent compound, **2m,** which was 11-folds more active than the former with an IC_{50} of 0.9 ± 0.1 μM (Table 3). In

2m, the presence of an electron donating methoxy group (R_3) in the 4'-position of the phenyl helps to increase the hydrophobicity of the aromatic centroid which is attached at the 4th position of the thiazole ring (Fig. 4d) and thus might be responsible for the high enzyme inhibition. Docking studies which is discussed later also suggest that the methoxy group could be potentially involved in the ionic interactions (H-bond acceptor and donor) with the carbonyl groups of the amino acids, Ile673, Val175 and Phe177, in the lipophilic side chain of the protein. The inhibitory activity of **2m** is better than that of the standard drug, Zileuton (IC_{50} = 1.5 ± 0.3 µM) (Table 3). SAR studies indicate that when methoxy is replaced with nitro, **2n** (79.6 ± 1.5 % at 10 µM), (Table 1) the activity decreases by one fold which might be due to the decrease in the electron density at the *p*-position of the aromatic ring through a resonance withdrawing effect of the nitro group. Removal of methoxy or nitro group (R_3 = H, i.e. without any substituent), results in a 50 % reduction in the activity (compound **2g**: 48.6 ± 0.7 %). Insertion of another bulky 2^0 amine (N-phenyl piperazine) at the 2nd position of the thiazole ring, does not alter the efficiency against 5-LOX (compound **2f**: 38.3 ± 2.9 %). Nevertheless, further variation in the substituents at the R_3 by –OCH_3, **2l** (53.1 ± 2.9 %) and –NO_2, **2j** (67.8 ± 1.5 %) increases the potency by 1.5 to 1.8 times when compared to **2f** (Table 1). Surprisingly, there is a large increase in the potency when R_3 = H is retained and bulky 2^0 amine group at the 2nd position of the thiazole ring (R_1 & R_2) is exchanged by smaller 2^0 amines such as piperidine, **2a** (IC_{50} = 3.1 ± 0.1 µM) or morpholine, **2b** (IC_{50} = 2.3 ± 0.2 µM) (Table 3). However, these smaller 2^0 amines are not tolerated by any electron donating (-OCH_3) or withdrawing group (fluoro) at the R_3 position. Thus, a considerable loss in potency is seen in **2h** (62.0 ± 9.4 %) and **2k** (50.2 ± 4.4 %). Therefore, sustaining R_3 = H and decreasing the bulkiness of 2^0 amine (R_1 and R_2) yields analogues, **2d, 2e** and **2c,** with high activity. Compared to substituent, N-methyl benzyl amine,

2d (53.1 ± 1.5 %), the N-methyl aniline analogue, **2e** (67.8 ± 2.9 %) is more potent. Insertion of an electron donating group such as methoxy at R_3 in **2d** leads to a considerable decrease in the potency (compound **2i**: 17.7 ± 2.9 %). **2c** (75.3 ± 3.8 %), with a smaller 2^0 amine (pyrrolidine) substitution when compared to that in **2d** leads to 1.5 times more activity (Table 1).

Table 2: 5-LOX inhibition and antioxidant activities of 4-substituted-N-(amino-1-carbonothioyl)benzamide derivatives (**3a-q**). Data are expressed as means ± SD obtained from three independent experiments.

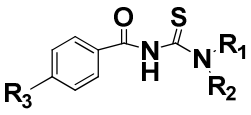

S.No.	Compd code	Structure	% 5-LOX Inhibition ± SD (10 µM)	% scavenging of DPPH ± SD (20 µM)
15	3a	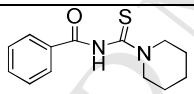	56.8 ± 2.3	23.7 ± 0.7
16	3b	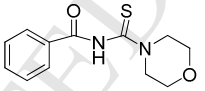	79.4 ± 1.7	19.1 ± 1.6
17	3c	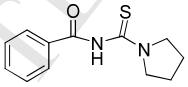	24.5 ± 4.5	25.6 ± 2.8
18	3d	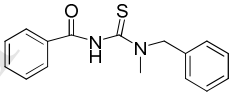	80.7 ± 3.8	18.4 ± 0.9
19	3e	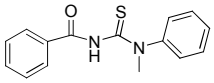	78.7 ± 2.8	13.2 ± 0.4
20	3f	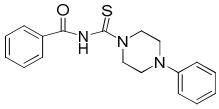	91.3 ± 3.8	24.1 ± 0.7
21	3g	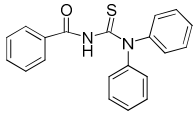	73.3 ± 6.6	11.3 ± 1.6
22	3h	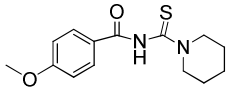	86.0 ± 1.9	21.8 ± 0.7
23	3i	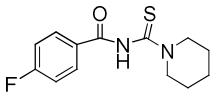	80.7 ± 3.8	5.9 ± 0.9

24	**3j**	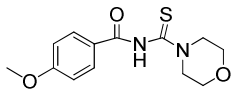	68.3 ± 7.2	3.9 ± 0.1
25	**3k**	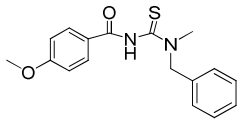	26.5 ± 1.5	7.4 ± 0.2
26	**3l**	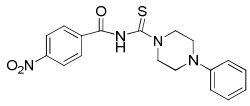	76.6 ± 1.5	20.3 ± 3.5
27	**3m**	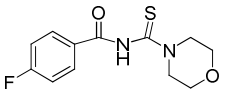	29.5 ± 5.9	9.1 ± 1.3
28	**3n**	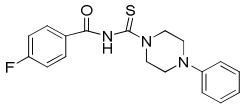	23.6 ± 2.9	6.3 ± 0.9
29	**3o**	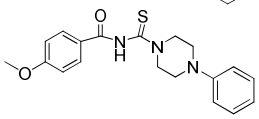	36.8 ± 2.2	3.7 ± 0.7
30	**3p**	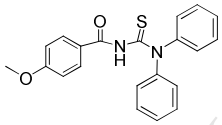	19.2 ± 5.2	8.1 ± 3.5
31	**3q**	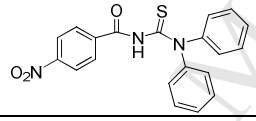	30.9 ± 3.7	4.7 ± 5.3

Another set of analogues with thiourea as the basic moeity (**3**) with different secondary amines (at R_1 and R_2 positions) are synthesized retaining the presence of benzoyl (H-bond acceptor property) group which is critical for activity. The highly potent compound in this series, **3f**, (Table 3) with bulkiest 2^0 amine (phenyl piperazine) substitution replacing R_1 and R_2 while benzoyl having no substitution (R_3 = H) showed an IC_{50} of 1.4 ± 0.1 µM (91.3 ± 3.8 % at 10 µM) against 5-LOX. This activity is found to be approximately similar to the standard drug, Zileuton (IC_{50} = 1.5 ± 0.3 µM). Replacement of hydrogen (R_3) at the *para*-position of the benzoyl ring with an electron withdrawing groups such as nitro, **3l** (76.6 ± 1.5 %) showed a marginal reduction in the potency whereas considerable loss in inhibitory activity is observed with fluoro, **3n** (23.6 ± 2.9 %) (Table 2). An electron donating methoxy group, **3o** (36.8 ± 2.2 %) also could not improve the potency. Bulky 2^0 amines such as benzyl methyl amine, **3d**, or methyl

aniline, **3e**, or diphenyl amine, **3g,** showed high inhibitory activities (of 80.7 ± 3.8 %, 78.7 ± 2.8 % and 73.3 ± 6.6 % respectively). A drastic loss in potency is observed when hydrogen at R_3 in **3d** is substituted with methoxy group producing **3k** (26.5 ± 1.5 %). Similar effects are observed with methoxy analogue, **3p** (19.2 ± 5.2 %), and nitro analogue, **3q** (30.9 ± 3.7 %). However, exchanging bulkier amine with smaller 2^0 amines such as piperidine in **3o** led to a significantly improved compound, **3h**, with an IC_{50} of 3.3 ± 0.2 µM. There is little change in activity when methoxy is replaced with fluoro substituent, **3i** (IC_{50} = 3.8 ± 0.2 µM). But removal of either of the two substituents, (R_3 = H), led to a drop in the potency (compound **3a**).

Table 3: IC_{50} values of the best six analogues against 5-LOX enzyme in cell free assay, their pseudoperoxidase activity and mechanism of action.

Compd code	Structure	5-LOX inhibition, IC_{50} (µM)	% Redox absorbance (at 10 µM of 13(S)-HpODE and inhibitor)	Type of mechanism
2a	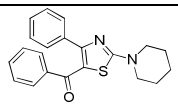	3.1 ± 0.1	+ 0.6	Non-redox
2b	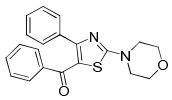	2.3 ± 0.2	+ 2.1	Non-redox
2m	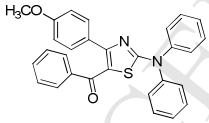	0.9 ± 0.1	+ 29.4	Non-redox (Competitive)
3f	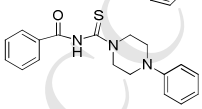	1.4 ± 0.1	- 46.2	Redox (Non-competitive)
3h	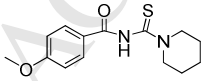	3.3 ± 0.2	- 35.3	Redox
3i	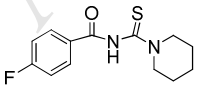	3.8 ± 0.2	nd	nd
Zileuton	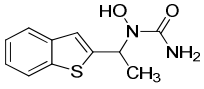	1.5 ± 0.3	- 49.6	Redox

'-' indicates % decrease in absorbance due to consumption of 13(S)-HpODE
'+' indicates % increase in absorbance
nd - not determined

2.6. Kinetics of 5-LOX inhibition

A steady-state enzyme kinetic analysis of these two most active inhibitors (**2m** and **3f**) was performed at three different concentrations (0, 5 and 10 µM) in the presence of different concentrations of the substrate (AA) to determine the initial rate [30,32]. The Lineweaver-Burke plot for the compound **2m** shows that all the lines intersect on the y-axis indicating, it acts as a competitive inhibitor (Figure 5a). The value of Vmax was found to be constant at these three concentrations (0.39 ± 0.02, 0.38 ± 0.02, 0.38 ± 0.01 nmol/min) whereas the Km values increased (0.42 ± 0.15, 0.99 ± 0.26, 1.51 ± 0.20 µM) with increasing concentration of **2m**. Lineweaver–Burk plot for the other compound, **3f,** shows that all the three lines are intersecting in the left hand side of the y-axis (Fig. 5b). Also Vmax (0.48 ± 0.02, 0.40 ± 0.01, 0.34 ± 0.01 nmol/min) decreases while Km values are almost constant (0.7761 ± 0.22, 0.7904 ± 0.13, 0.7674 ± 0.09 µM) for increasing concentration of **3f** indicating non-competitive (mixed) type of inhibition where inhibitor may be binding to both the free enzyme and the enzyme-substrate complex.

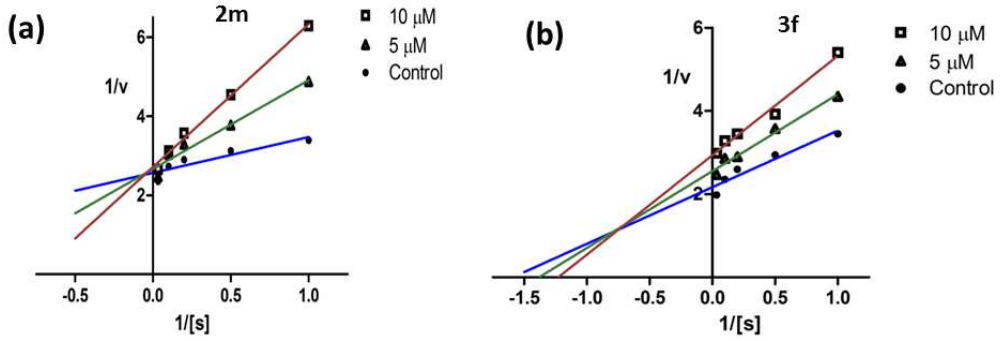

Fig. 5: The Lineweaver-Burk plots for compounds a) **2m** tested at 5 and 10 µM concentrations and b) **3f** tested at concentrations 5 and 10 µM. [S] = Substrate (AA) concentration, V = Velocity of reaction. Control (no inhibitor, 0 µM).

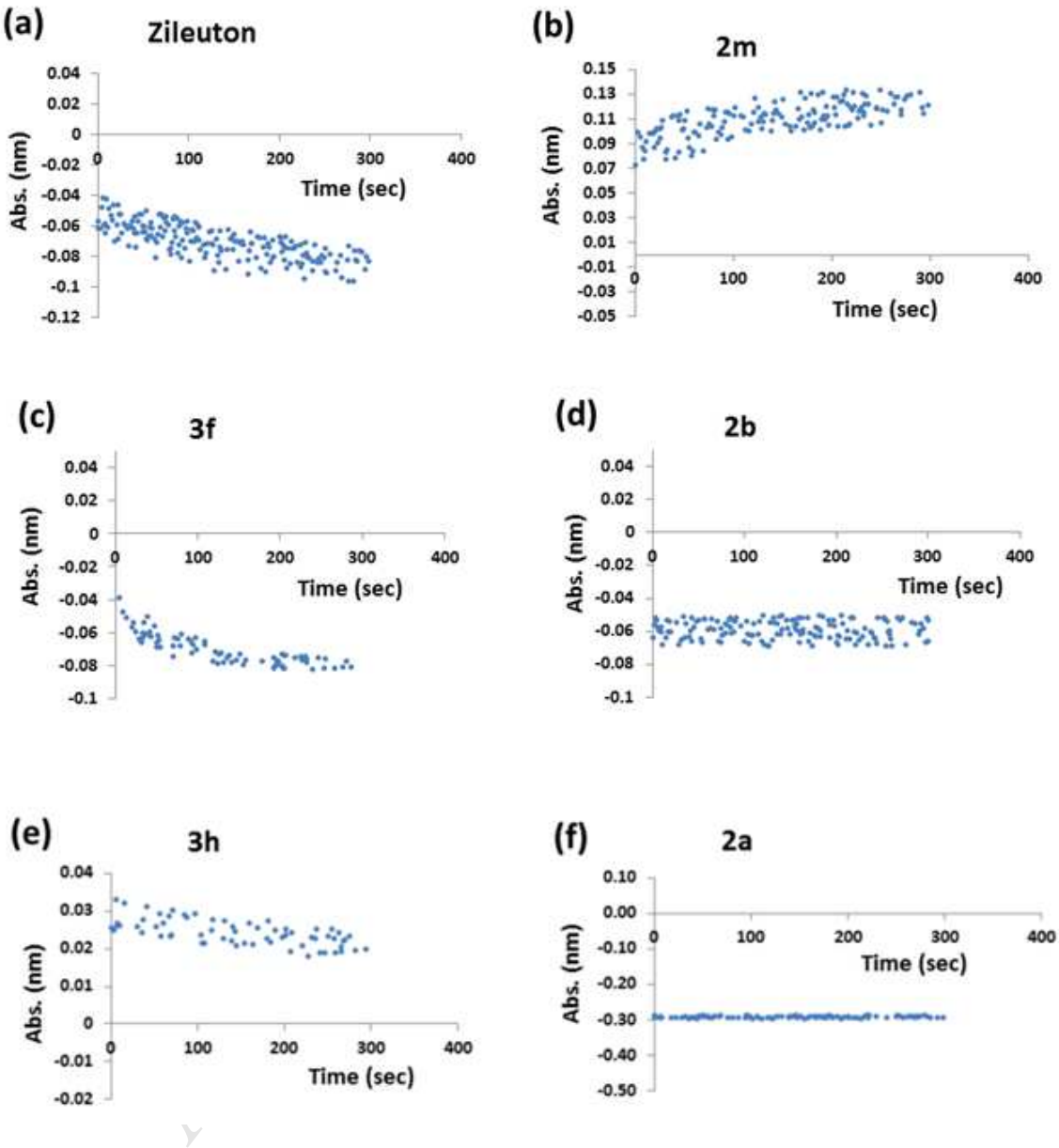

Fig. 6: Pseudoperoxidase activity plot (absorbance measured at 234 nm substracted from control) showing amount of consumption of 13(S)-HpODE by a) Zileuton, b) **2m** c) **3f**, d) **2b**, e) **3h**, f) **2a**.

2.7. Pseudoperoxidase activity and redox mechanism

Competitive (non-redox), redox and iron chelating are three well-known reported mechanisms through which compounds inhibit the 5-LOX enzyme [8,33]. Moreover, competitive inhibitors bind to the active site of the enzyme while iron chelators chelate the metal iron thereby, blocking the active site and thus exhibit the inhibitory activity. In contratst, redox inhibitors act by converting the active form of iron to inactive state by redox process and hence inhibit the activity of the enzyme [34]. 5-LOX is a non-heme iron containing enzyme having Fe^{3+} ion in the activated form which is reduced to Fe^{2+} in the presence of a redox inhibitor. Inactivated ferrous ion can consume lipid peroxide to reactivate the redox cycle of the enzyme. In the pseudoperoxidase activity assay, the consumption of 13(S)-hydroperoxyoctadecadienoic acid (13(S) HpODE) in the presence of an inhibitor is determined which is a measure of the redox potential of the inhibitor [35].

Redox inhibitory activities of **2m, 2a, 2b, 3f** and **3h** are elucidated here. The decrease in the amount of peroxide substrate, 13(S) HpODE is determined at 234 nm (Fig. 6). The best 5-LOX inhibitor, **3f**, is found to decrease the absorbance by 46.2 % in 300 s (Table 3, Fig. 6c) indicating significant degradation of the hydroperoxide product, thus suggesting its redox behaviour. While Zileuton, a known redox 5-LOX inhibitor shows 49.6 % degradation of the hydroperoxide (Fig. 6a). Compound **3h** also shows considerable degradation of the peroxide (35.3 %) indicating that it also disrupts the redox cycle of the enzyme. While **2m** does not decrease the absorbance (indicating that it does not disturb the redox cycle) (Fig. 6b). However, the graph shows an increase in the absorbance as afunction of time. This increase might be due to an unknown reaction in the assay mixture leading to UV absorbance at the same wavelength in the absence of redox activity or compound itself exhibiting UV characterisitcs. Also, when compound **2m** alone

is tested without the enzyme at the same wavelength, an increase in the absorbance is observed as a function of time. Similar increase in absorbance is reported in literature while performing pseudoperoxidase activity which is attributed to the above mentioned reasons [36,37]. This compound does not exhibit redox activity and probably binds to the active site of the enzyme as a competitive inhibitor as seen from the L-B plot (Fig. 5a). Compounds, **2a** and **2b** did not show any considerable reduction in the absorbance with time (Fig. 6d, f). So they may be inhibiting the enzyme through non-redox mechanism.

2.8. DPPH radical scavenging activity

There is a close relationship between a 5-LOX inhibitor and its radical scavenging property because several of them are known to change the oxidation state of the iron from ferric (Fe^{3+}) to ferrous (Fe^{2+}) present in the enzyme [38]. Radical scavenging activity of all the compounds at 20 µM is determined by using free radical, 2, 2-diphenyl-1-picrylhydrazyl (DPPH) assay method [39]. Ascorbic acid is used as the standard which exhibited 84.1 ± 0.5 % antioxidant activity at 20 µM (Table 1). Most of the compounds from both the series showed poor radical scavenging property, whereas **3f** and **3h** showed 24.1 ± 0.7 and 21.8 ± 0.7 % activity respectively (Table 2). Pseudoperoxidase activity also indicates that these compounds act on the enzyme through the redox mechanism. While, Zileuton exhibited 17.8 ± 1.2 % free radical scavenging activity (Table 2), compounds **2m**, **2a** and **2b** showed relatively lower antioxidant activities (11.8 ± 2.1, 8.5 ± 0.2 and 9.5 ± 0.7 % respectively) indicating that they probably act through a non-redox mechanism. Pseudoperoxidase activity assay also indicates that these three compounds do not follow the redox mechanism. L-B plot has also clearly revealed that compound **2m** acts through the competitive mode of inhibition.

2.9. Molecular docking studies

The experimental studies indicated that compounds **2m**, **2a** and **2b** act as competitive inhibitors so these ligands were docked into the active site of the enzyme, 5-LOX to understand their mode of binding and interaction they made with the active site amino acid residues. The docking was not performed for the compound **3f** which was found to be acting through non-competitive mode. The crystal structure of the protein (pdb ID 3o8y) was obtained from Brookhaven Protein Data Bank (PDB) and docking was performed with Molecular Operating Environment (MOE 2016.0801) software. Compound **2m** showed several interactions with the active site residues with a binding score of -7.0 kcal/mol (Fig. 7). The $–OCH_3$ group of the phenyl linker attached to the 4^{th} position of the thiazole ring interacts with Ile673 (3.74 Å), Val175 (4.11 Å) and Phe177 (3.69 Å) in the hydrophobic pocket of the protein through H-bond. 2^0 amine containing phenyl groups are also seen to make H-bonds with Asn187 (3.75 Å), Lys183 (4.21 Å) and Phe610 (4.09 Å). Polar amino acid residues such as Gln609 and Asn180 are observed to possess pi-H interactions with one of the phenyl ring of 2^0 amine and benzoyl ring respectively (Fig. 7).

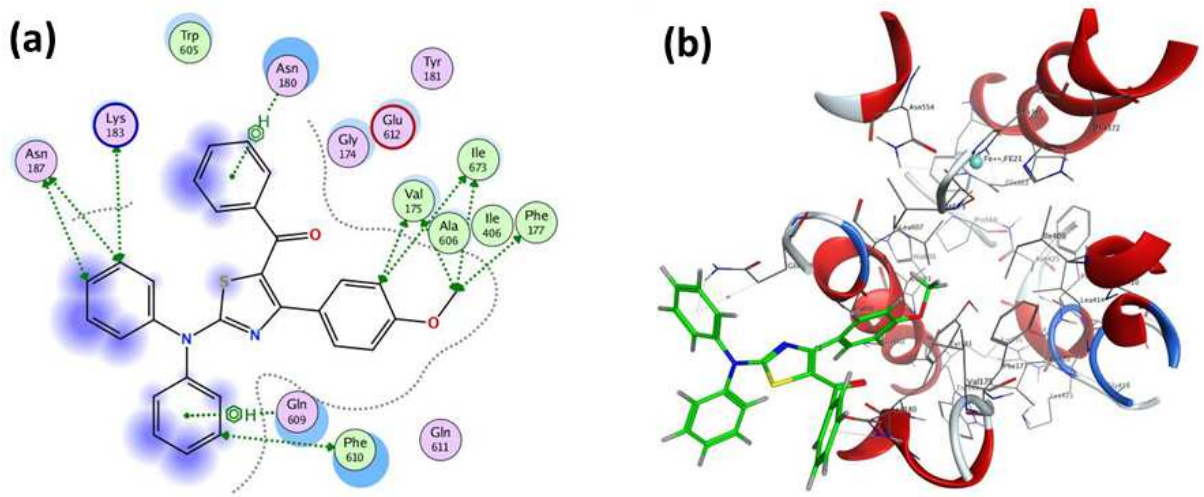

Fig. 7: Binding of compound **2m** with 5-LOX. (a) Ligplot showing residues involved in the interaction between the amino acids of the enzyme with compound **2m**. (b) Docked pose of compound **2m** in a stick model. Interactions are shown by dotted lines. Colours: carbon: grey, hydrogen: cyan, nitrogen: blue, sulphur: yellow, fluorine: green and oxygen: red.

Molecular docking of **2a** also showed appreciable interactions in the active site of 5-LOX with binding score of -5.1 kcal/mol. Side chain H-bond interactions between piperidine ring and Ile673 (3.99 Å), Val175 (3.91 Å) and Asn180 (3.63 Å) and between hydrogen of phenyl ring at the 4th position of thiazole moiety and carbonyl of Asn187 (3.86 Å) are observed. This side chain phenyl ring also exhibits arene pi-H interaction with Lys183. Similar type of pi-H interaction is also seen with benzoyl group and Asn180 (Fig. 8).

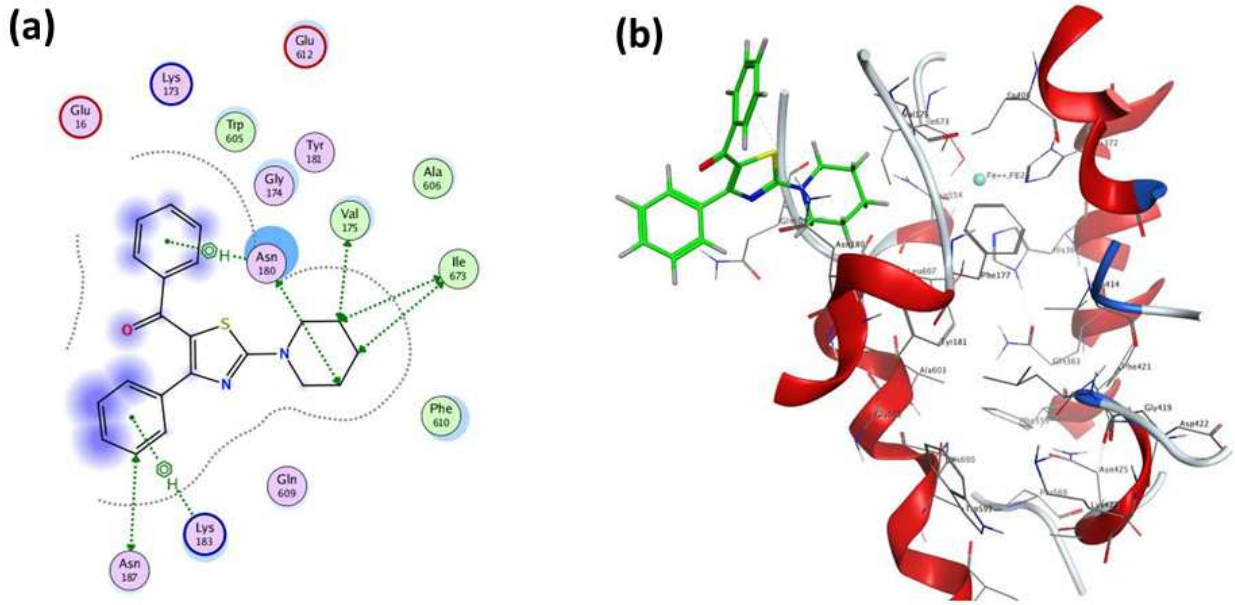

Fig. 8: Binding of compound **2a** with 5-LOX. (a) Ligplot showing residues involved in the interaction between the amino acids of the enzyme with compound **2a**. (b) Docked pose of compound **2a** in a stick model. Interactions are shown by dotted lines. Colours: carbon: grey, hydrogen: cyan, nitrogen: blue, sulphur: yellow, fluorine: green and oxygen: red.

Compound **2b** with a docking score of -5.3 kcal/mol is found to possess side chain H-bond interactions with morpholine and Ile673 (3.96, 3.70 Å) and Val175 (3.99, 3.48 Å). Also, a back bone H-bond donor is detected between sulphur of thiazole ring and Gly174 (3.49 Å) (Fig. 9). These computational studies indicate that these compounds (competitive and non-redox mode) bind effectively through H-bond and pi-H interactions with the amino acid residues in the active site of the enzyme.

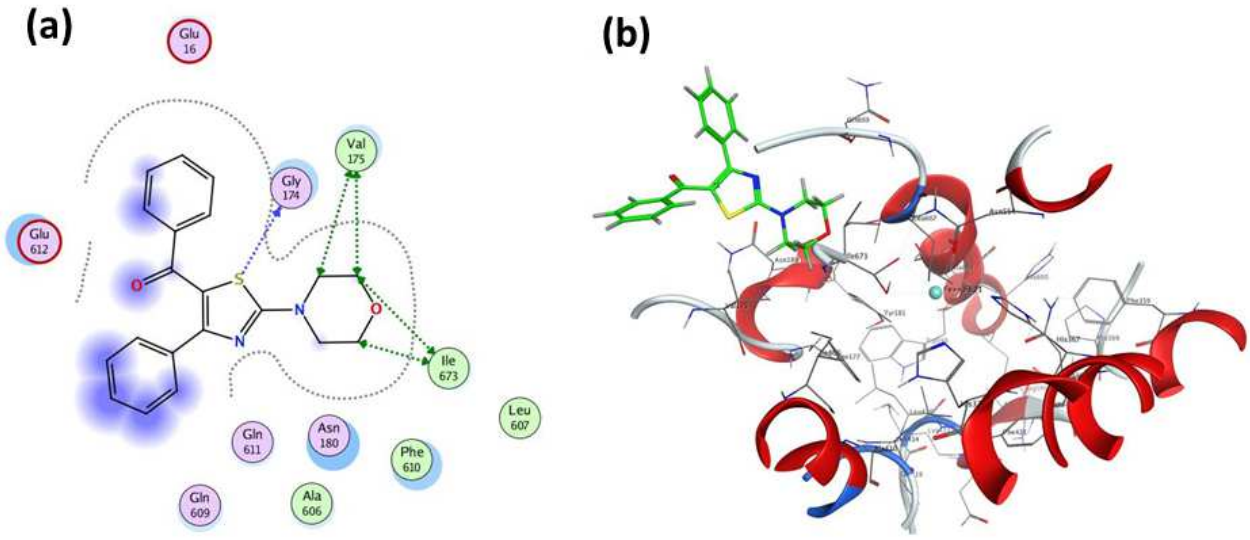

Fig. 9: Binding of compound **2b** with 5-LOX. (a) Ligplot showing residues involved in the interaction between the amino acids of the enzyme with compound **2b**. (b) Docked pose of compound **2b** in a stick model. Interactions are shown by dotted lines. Colours: carbon: grey, hydrogen: cyan, nitrogen: blue, sulphur: yellow, fluorine: green and oxygen: red.

2.10. Pan-Assay Interference Compounds (PAINS)

Chemical compounds which react non-specifically with multiple biological targets and often depict false positives in high throughput screenings and they are interpreted as PAINS. On the contrary, a selective inhibitor or drug-like molecule will interact specifically with the target

protein. But These PAINS show activity in many assays because of probably due to covalent modifications, chelation, autofluorescence, agglomeration or degradation of the target protein [40]. Many classes of compounds have been categorized as PAINS including rhodanines, isothiazolones, enones, and quinones [41,42]. So it is important to determine if compounds that are being studied as drug candidates posses these structural features which may lead to them to be classified as PAINS. The currently synthesized thiazoles and thioureas were tested using ZINC15 database and found to be PAINS negative.

3. Conclusion

5-LOX is an important target in the leukotriene pathway which is implicated in asthma and other inflammatory disorders. The drug, Zileuton, is withdrawn from the market due to its non-selective nature. In the present study, novel inhibitors of the enzyme 5-LOX, were designed using pharmacophore modeling technique, and then chemically synthesized (31 compounds) and tested against this enzyme. Out of 31 compounds synthesized, 19 compounds (**2d, 2f, 2g, 2i, 2j, 2k, 2l, 2m, 2n, 3d, 3f, 3h, 3i, 3k, 3l, 3m, 3n, 3o, 3p**) are completely novel as verified by Scifinder and for other 12 compounds (**2a, 2b, 2c, 2e, 2h, 3a, 3b, 3c, 3e, 3g, 3j, 3q**), no reports are available for their biological activity against 5-LOX in literature. Our previous studies identified a thiazole inhibitor (**1,** IC_{50} ~10 µM). Introduction of hydrophobic and H-bond acceptor properties in the molecule (**1**) by incorporating a benzoyl group at the 5^{th} and substituted secondary (2^0) amine at the 2^{nd} positions respectively in the basic thiazole moiety provided a potent analogue (**2m)** with an IC_{50} of 0.9 ± 0.1 µM. This compound is found more potent than the drug, Zileuton (IC_{50} = 1.5 **±** 0.3 µM). Another compound (**3f)** exhibited an IC_{50} of 1.4 ± 0.1 µM. Structure activity relationship studies revealed that the presence of electron

donating groups such as methoxy (**2m**) at 4'- position along with nitrogen containing groups, 2^0 amine as bulky side chain in scaffold (**2**) increases the hydrophobicity in the molecule and thus leads to high inhibitory potency. In contrast, a bulky 2^0 amine side chain in moiety (**3**) does not require any substitution at R_3 position (**3f**) to possess high potency. Pharmacophore studies also indicated that the presence of hydrophobic and H-bond acceptor is essential for the enzyme inhibition (Figure 4). Additional experiments such as pseudoperoxidase, kinetic and antioxidant assays gave a clear picture that the best compound, **2m,** acts through a competitive mode of inhibition (non-redox process). **3f,** on the other hand acts by non-competitive (redox) mechanism. This compound also has high antioxidant activity. Computational analysis was in good agreement with the experimental data. The non-redox inhibitors, **2a, 2b and 2m**, interact with the protein through H-bond and pi-H interactions in the active site (Fig. 7). Highly potent both redox and non-redox type of 5-LOX inhibitors are reported here which could act as novel chemical entities for further development as an anti-inflammatory drugs.

4. Experimental

4.1. General

All solvents and reagents were purchased from chemical suppliers Sigma-Aldrich Chemie GmbH (Steinheim, Germany), Alfa-Aesar GmbH & Co. (Heysham, England), Acros Organics (Geel, Belgium) and Thermo Fisher Scientific (Waltham, United States) and were used without further purification. ^{1}H and ^{13}C NMR spectra were obtained on Bruker AVANCE III 500 MHz (AV-500) NMR Spectrometer using $CDCl_3$ and DMSO-d_6 as solvents with tetramethylsilane (TMS) as an internal standard. Chemical shifts (δ) are expressed in parts per million (ppm) and coupling constants (J) values are expressed in hertz (Hz) unit. High resolution mass spectra

(HRMS) were recorded on Thermo Scientific Orbitrap Elite Mass spectrometer equipped with dual pressure linear ion trap coupled with high-field orbitrap Mass analyzer. IR spectra were recorded on Perkin Elmer Spectrum1 FT-IR instrument with a resolution of 1.0 cm^{-1} and MIR 450-4000 cm^{-1}. Melting points were recorded in capillaries on GUNA melting point apparatus and are uncorrected. Synthetic reactions were monitored by thin layer chromatography (TLC) on TLC Silica gel 60G F_{254} plates from Merck KGaA (Darmstadt, Germany), Millipore. Column chromatography was performed using 60−120 mesh silica. Visualization of compounds was done using UV light or iodine chamber. Purities of all title compounds synthesized here were 95 % or higher.

4.1.1. General procedure for the synthesis of compounds ***3a-q****.* Substituted benzoyl chloride (1.5 mmol) in 10 mL toluene was added to a mixture of aqueous solution of potassium thiocyanate (1.9 mmol) and cetrimide (Scheme 1). The reaction mixture was stirred for 2 h at room temperature. Aromatic yellow layer was separated from aqueous layer. N,N-dialkylamines (1.5 mmol) was added to the aromatic layer at 0 ^{0}C and stirred at room temperature for 3-4 h. The solid obtained was filtered and the crude product was washed with saturated aqueous sodium bicarbonate solution, dried in vacuo and further recrystallized with ethanol/ethyl acetate to obtain pure products.

*4.1.1.1. N-(piperidine-1-carbonothioyl)benzamide (****3a****).* Cream solid, yield 74 %, mp 114-115 ^{0}C. IR (KBr, cm^{-1}) 3439 (N-H str), 3168 (aromatic C-H str), 1650 (amide C=O str), 1580 (N-H bend), 1530 (aromatic C=C str), 1250 (aromatic amine C-N str). ^{1}H NMR (500 MHz, $CDCl_3$) δ: 8.46 (s, 1H, NH), 7.86 (d, J = 7.2 Hz, 2H, Ar-H), 7.60 (t, J = 7.4 Hz, 1H, Ar-H), 7.50 (t, J = 7.7 Hz, 2H, Ar-H), 4.19 (s, 2H, piperidin-H), 3.62 (s, 2H, piperidin-H), 1.84 – 1.73 (m, 6H, piperidin-H). ^{13}C NMR (126 MHz, $CDCl_3$) δ: 178.25, 163.19, 132.94, 132.62, 128.82, 127.82,

53.05, 52.77, 26.04, 25.25, 23.66. HRMS (ESI) *m/z* for $C_{13}H_{16}N_2OS$ $[M + Na]^+$ calcd 271.0876, found 271.0880.

4.1.1.2. N-(morpholine-4-carbonothioyl)benzamide (***3b***). White solid, yield 67 %, mp 124-126 ^{0}C. IR (KBr, cm^{-1}) 3452, 3243 (N-H str), 3021 (aromatic C-H str), 1665 (amide C=O str), 1580 (N-H bend), 1523 (aromatic C=C str), 1269 (aromatic amine C-N str), 1114 (morpholine C-O-C str). ^{1}H NMR (500 MHz, $CDCl_3$) δ: 8.61 (s, 1H, NH), 7.86 (d, J = 7.7 Hz, 2H, Ar-H), 7.61 (t, J = 7.4 Hz, 1H, Ar-H), 7.50 (t, J = 7.6 Hz, 2H, Ar-H), 4.25 (s, 2H, morpholin-H), 3.85 (s, 4H, morpholin-H), 3.68 (s, 2H, morpholin-H). ^{13}C NMR (126 MHz, $CDCl_3$) δ: 179.34, 163.34, 133.18, 132.32, 128.97, 127.83, 66.23, 52.51, 51.60. HRMS (ESI) *m/z* for $C_{12}H_{14}N_2O_2S$ $[M + Na]^+$ calcd 273.0668, found 273.0670.

*4.1.1.3. N-(pyrrolidine-1-carbonothioyl)benzamide (**3c**).* White solid, yield 64 %, mp 120-123 ^{0}C. IR (KBr, cm^{-1}) 3442 (N-H str), 3145 (aromatic C-H str), 1644 (amide C=O str), 1579 (N-H bend), 1537 (aromatic C=C str), 1253 (aromatic amine C-N str). ^{1}H NMR (500 MHz, $CDCl_3$) δ: 8.56 (s, 1H, NH), 7.81 (d, J = 7.7 Hz, 2H, Ar-H), 7.55 (t, J = 7.4 Hz, 1H, Ar-H), 7.44 (t, J = 7.6 Hz, 2H, Ar-H), 3.85 (t, J = 7.0 Hz, 2H, pyrrolidin-H), 3.67 (t, J = 6.7 Hz, 2H, pyrrolidin-H), 2.05 – 1.99 (m, 2H, pyrrolidin-H), 1.98 – 1.92 (m, 2H, pyrrolidin-H). ^{13}C NMR (126 MHz, $CDCl_3$) δ: 176.59, 163.51, 133.13, 132.76, 129.03, 128.11, 54.72, 53.10, 26.43, 24.84. HRMS (ESI) *m/z* for $C_{12}H_{14}N_2OS$ $[M + H]^+$ calcd 235.0900, found 235.0900.

*4.1.1.4. N-(benzyl(methyl)carbamothioyl)benzamide (**3d**).* Cream solid, yield 93 %, mp 112-115 ^{0}C. IR (KBr, cm^{-1}) 3450, 3186 (N-H str), 3071 (aromatic C-H str), 2926 (methyl C-H str), 2892 (CH_2 C-H str) 1682 (amide C=O str), 1580 (N-H bend), 1539 (aromatic C=C str), 1483 (C-H sp^3 bend), 1260 (amine C-N str). ^{1}H NMR (500 MHz, $CDCl_3$) δ: 8.60 (s, 1H, NH), 7.90 (d, J = 7.5

Hz, 2H, Ar-H), 7.61 (t, *J* = 6.9 Hz, 1H, Ar-H), 7.56 – 7.44 (m, 4H, Ar-H), 7.41 (t, *J* = 7.3 Hz, 2H, Ar-H), 7.34 (t, *J* = 7.2 Hz, 1H, Ar-H), 5.31 (s, 1H, CH_2), 4.82 (s, 1H, CH_2), 3.35 (s, 1H, N-CH_3), 3.19 (s, 2H, N-CH_3). ^{13}C NMR (126 MHz, $CDCl_3$) *δ*: 181.54, 163.52, 134.86, 133.08, 132.51, 128.93, 128.83, 127.94, 127.88, 59.65, 40.37. HRMS (ESI) *m/z* for $C_{16}H_{16}N_2OS$ $[M + Na]^+$ calcd 307.0876, found 307.0880.

*4.1.1.5. N-(methyl(phenyl)carbamothioyl)benzamide (**3e**).* Light yellow solid, yield 84 %, mp 117-119 ^{0}C. IR (KBr, cm^{-1}) 3455, 3195 (N-H str), 3029 (aromatic C-H str), 2932 (methyl C-H str), 1695 (amide C=O str), 1597 (N-H bend), 1515 (aromatic C=C str), 1436, 1382 (C-H sp^3 bend), 1261 (amine C-N str). ^{1}H NMR (500 MHz, $CDCl_3$) *δ*: 8.45 (s, 1H, NH), 7.52 (dd, *J* = 24.9, 17.9 Hz, 3H, Ar-H), 7.42 – 7.34 (m, 7H, Ar-H), 3.78 (s, 3H, N-CH_3). ^{13}C NMR (126 MHz, $CDCl_3$) *δ*: 180.55, 162.84, 145.29, 132.92, 132.67, 129.46, 128.73, 127.90, 127.55, 125.54, 45.59. HRMS (ESI) *m/z* for $C_{15}H_{14}N_2OS$ $[M + H]^+$ calcd 271.0900, found 271.0900.

*4.1.1.6. N-(4-phenylpiperazine-1-carbonothioyl)benzamide (**3f**).* Cream solid, yield 75 %, mp 122-125 ^{0}C. IR (KBr, cm^{-1}) 3434, 3259 (N-H str), 3058 (aromatic C-H str), 1668 (amide C=O str), 1599 (N-H bend), 1532 (aromatic C=C str), 1273, 1221, 1161 (amine C-N str). ^{1}H NMR (500 MHz, $CDCl_3$) *δ*: 8.58 (s, 1H, NH), 7.89 (d, *J* = 8.0 Hz, 2H, Ar-H), 7.63 (t, *J* = 7.2 Hz, 1H, Ar-H), 7.52 (t, *J* = 7.5 Hz, 2H, Ar-H), 7.32 (t, *J* = 7.6 Hz, 2H, Ar-H), 6.95 (dd, *J* = 12.5, 7.8 Hz, 3H, Ar-H), 4.40 (s, 2H, piperazine-H), 3.86 (s, 2H, piperazine-H), 3.40 (d, *J* = 22.6 Hz, 4H, piperazine-H). ^{13}C NMR (126 MHz, $CDCl_3$) *δ*: 179.18, 163.34, 150.35, 133.17, 132.41, 129.32, 129.00, 127.86, 120.56, 116.46, 51.65, 51.20, 48.96, 48.62. HRMS (ESI) *m/z* for $C_{18}H_{19}N_3OS$ $[M + H]^{--}$ calcd 326.1322, found 326.1321.

*4.1.1.7. N-(Diphenylcarbamothioyl)benzamide (**3g**).* Fluorescent yellow solid, yield 97 %, mp 113-115 ^{0}C. IR (KBr, cm^{-1}) 3431, 3220 (N-H str), 3064 (aromatic C-H str), 1691 (amide C=O str), 1591 (N-H bend), 1503 (aromatic C=C str), 1357, 1256 (amine C-N str). ^{1}H NMR (500 MHz, $CDCl_3$) δ: 8.59 (s, 1H, NH), 7.48 (d, J = 7.7 Hz, 4H, Ar-H), 7.38 (t, J = 7.3 Hz, 2H, Ar-H), 7.14 (dd, J = 8.6, 6.9 Hz, 6H, Ar-H), 6.96 (d, J = 8.2 Hz, 2H, Ar-H), 6.81 (t, J = 7.3 Hz, 1H, Ar-H). ^{13}C NMR (126 MHz, $CDCl_3$) δ: 182.45, 162.32, 145.72, 143.17, 132.82, 129.34, 129.30, 128.99, 128.80, 127.64, 127.47, 126.89, 120.99, 117.83. HRMS (ESI) *m/z* for $C_{20}H_{16}N_2OS$ [M + H]$^{--}$ calcd 333.1056, found 333.1052.

*4.1.1.8. 4-Methoxy-N-(piperidine-1-carbonothioyl)benzamide (**3h**).* Cream solid, yield 56 %, mp 122-124 ^{0}C. IR (KBr, cm^{-1}) 3283 (N-H str), 3054 (aromatic C-H str), 2939 (methyl C-H str), 1647 (amide C=O str), 1605 (N-H bend), 1528, 1434 (aromatic C=C str), 1264, 1186 (amine C-N str), 1024 (C-O str). ^{1}H NMR (500 MHz, $CDCl_3$) δ: 8.38 (s, 1H, NH), 7.83 (t, J = 9.9 Hz, 2H, Ar-H), 6.98 (dd, J = 17.9, 8.7 Hz, 2H, Ar-H), 4.18 (s, 2H, piperidin-H), 3.89 (d, J = 9.3 Hz, 3H, O-CH_3), 3.61 (s, 2H, piperidin-H), 1.76 (d, J = 33.8 Hz, 6H, piperidin-H). ^{13}C NMR (126 MHz, $CDCl_3$) δ: 182.53, 178.48, 165.91, 164.06, 163.38, 162.75, 129.91, 124.73, 123.44, 114.44, 114.12, 55.55, 53.08, 52.78, 26.06, 25.28, 23.89. HRMS (ESI) *m/z* for $C_{14}H_{18}N_2O_2S$ [M + H]$^{--}$ calcd 279.1162, found 279.1156.

*4.1.1.9. 4-Fluoro-N-(piperidine-1-carbonothioyl)benzamide (**3i**).* Fluorescent yellow solid, yield 41 %, mp 172-174 ^{0}C. IR (KBr, cm^{-1}) 3301, 3157 (N-H str), 1683 (amide C=O str), 1603 (N-H bend), 1536, 1503 (aromatic C=C str), 1231 (amine C-N str), 1008 (C-F str). ^{1}H NMR (500 MHz, $CDCl_3$) δ: 8.54 (s, 1H, NH), 7.88 (dd, J = 8.8, 5.2 Hz, 2H, Ar-H), 7.24 – 7.08 (m, 2H, Ar-H), 4.18 (s, 2H, piperidin-H), 3.60 (s, 2H, piperidin-H), 3.26 – 3.06 (m, 1H, piperidin-H), 1.89 (dt, J = 11.7, 5.9 Hz, 1H, piperidin-H), 1.77 (d, J = 41.6 Hz, 4H, piperidin-H). ^{13}C NMR (126

MHz, $CDCl_3$) δ: 178.06, 166.58, 164.55, 162.27, 130.47, 130.40, 128.76, 116.15, 115.98, 53.01, 52.77, 44.96, 26.05, 25.26, 23.84, 22.55, 22.20. HRMS (ESI) *m/z* for HRMS (ESI) *m/z* for $C_{13}H_{15}FN_2OS$ $[M + H]^{--}$ calcd 267.0962, found 267.0961.

*4.1.1.10. 4-Methoxy-N-(morpholine-4-carbonothioyl)benzamide (**3j**).* Cream solid, yield 53 %, mp 108-110 ^{0}C. IR (KBr, cm^{-1}) 3321 (N-H str), 3019 (aromatic C-H str), 2924 (methyl C-H str), 1658 (amide C=O str), 1610 (N-H bend), 1524, 1434 (aromatic C=C str), 1262, 1234 (amine C-N str), 1113 (morpholine C-O-C), 1028 (C-O str). ^{1}H NMR (500 MHz, $CDCl_3$) δ: 8.47 (s, 1H, NH), 7.82 (d, *J* = 8.9 Hz, 2H, Ar-H), 6.97 (d, *J* = 8.8 Hz, 2H, Ar-H), 4.25 (s, 2H, morpholin-H), 3.97 – 3.79 (m, 7H, morpholin-H and O-CH_3), 3.67 (s, 2H, morpholin-H). ^{13}C NMR (126 MHz, $CDCl_3$) δ: 182.53, 179.55, 165.91, 164.06, 163.56, 162.79, 129.95, 124.40, 123.44, 114.45, 114.21, 66.26, 55.58, 52.58, 51.63. HRMS (ESI) *m/z* for $C_{13}H_{16}N_2O_3S$ $[M + H]^{--}$ calcd 281.0954, found 281.0952.

*4.1.1.11. N-(Benzyl(methyl)carbamothioyl)-4-methoxybenzamide (**3k**).* White solid, yield 61 %, mp 142-144 ^{0}C. IR (KBr, cm^{-1}) 3450, 3189 (N-H str), 3070 (aromatic C-H str), 2940, 2845 (methyl C-H str), 1682 (amide C=O str), 1604 (N-H bend), 1543, 1487 (aromatic C=C str), 1393, 1357 (C-H sp^3 bend), 1253, 1222, 1187 (amine C-N str), 1024 (C-O str). ^{1}H NMR (500 MHz, DMSO-d_6) δ: 10.75 (s, 1H, NH), 7.97 (d, *J* = 8.7 Hz, 2H, Ar-H), 7.46 (d, *J* = 7.4 Hz, 2H, Ar-H), 7.39 (t, *J* = 7.6 Hz, 2H, Ar-H), 7.32 (t, *J* = 7.1 Hz, 1H, Ar-H), 7.04 (d, *J* = 8.8 Hz, 2H, Ar-H), 5.31 (s, 2H, N-CH_2), 3.84 (s, 3H, O-CH_3), 3.07 (s, 3H, N-CH_3). ^{13}C NMR (126 MHz, DMSO-d_6) δ: 183.13, 163.98, 163.10, 135.92, 131.06, 128.98, 127.84, 125.20, 114.14, 58.28, 55.97. HRMS (ESI) *m/z* for $C_{17}H_{18}N_2O_2S$ $[M + H]^+$ calcd 315.1162, found 315.1164.

*4.1.1.12. 4-Nitro-N-(4-phenylpiperazine-1-carbonothioyl)benzamide (**3l**).* Yellow solid, yield 40 %, mp 156-158 ^{0}C. IR (KBr, cm^{-1}) 3440 (N-H str), 1682 (amide C=O str), 1604 (N-H bend), 1596, 1543 (aromatic C=C str), 1504 (nitro N-O str), 1291, 1229, 1145 (amine C-N str). ^{1}H NMR (500 MHz, DMSO-d_6) δ: 8.30 (d, J = 8.9 Hz, 1H, Ar-H), 8.16 (d, J = 8.9 Hz, 1H, Ar-H), 7.23 (dd, J = 16.1, 7.7 Hz, 3H, Ar-H), 6.95 (t, J = 8.7 Hz, 3H, Ar-H), 6.81 (td, J = 7.3, 3.9 Hz, 1H, Ar-H), 4.07 (s, 1H, NH), 3.26 (s, 2H, piperazine-H), 3.20 – 3.17 (m, 3H, piperazine-H), 3.07 – 3.04 (m, 3H, piperazine-H). ^{13}C NMR (126 MHz, DMSO-d_6) δ: 182.76, 177.28, 163.60, 151.36, 150.82, 149.46, 141.68, 130.20, 129.45, 123.70, 119.74, 119.66, 116.11, 115.98, 49.11, 48.36, 47.98, 44.75. HRMS (ESI) *m/z* for $C_{18}H_{18}N_4O_3S$ $[M + H]^{--}$ calcd 371.1172, found 371.1169.

*4.1.1.13. 4-Fluoro-N-(morpholine-4-carbonothioyl)benzamide (**3m**).* Cream solid, yield 47 %, mp 125-126 ^{0}C. IR (KBr, cm^{-1}) 3350 (N-H str), 3022 (aromatic C-H str), 2950, 1675 (amide C=O str), 1608 (N-H bend), 1547, 1482 (aromatic C=C str), 1250 (amine C-N str), 1120 (morpholine C-O-C), 1010 (C-F str). ^{1}H NMR (500 MHz, $CDCl_3$) δ: 8.62 (s, 1H, NH), 7.88 (dd, J = 8.6, 5.2 Hz, 2H, Ar-H), 7.18 (t, J = 8.5 Hz, 2H, Ar-H), 4.25 (s, 2H, morpholin-H), 3.85 (d, J = 28.4 Hz, 4H, morpholin-H), 3.66 (s, 2H, morpholin-H). ^{13}C NMR (126 MHz, $CDCl_3$) δ: 179.11, 166.71, 164.68, 162.29, 130.50, 130.43, 128.44, 116.27, 116.09, 66.21, 52.51, 51.56. HRMS (ESI) *m/z* for $C_{12}H_{13}FN_2O_2S$ $[M + H]^{+}$ calcd 269.0755, found 269.0755.

*4.1.1.14. 4-Fluoro-N-(4-phenylpiperazine-1-carbonothioyl)benzamide (**3n**).* White solid, yield 41 %, mp 148-150 ^{0}C. IR (KBr, cm^{-1}) 3429, 3260 (N-H str), 3048 (aromatic C-H str), 1662 (amide C=O str), 1587 (N-H bend), 1522 (aromatic C=C str), 1270, 1211 (amine C-N str), 1013 (C-F str). ^{1}H NMR (500 MHz, $CDCl_3$) δ: 7.91 (dd, J = 8.8, 5.2 Hz, 2H, Ar-H), 7.32 (dd, J = 8.7, 7.3 Hz, 2H, Ar-H), 7.20 (t, J = 8.6 Hz, 2H, Ar-H), 6.95 (t, J = 8.8 Hz, 3H, Ar-H), 4.40 (s, 2H,

piperazine-H), 3.84 (s, 2H, piperazine-H), 3.39 (d, *J* = 33.5 Hz, 4H, piperazine-H). ^{13}C NMR (126 MHz, $CDCl_3$) *δ*: 179.03, 166.71, 164.68, 162.39, 150.30, 130.52, 130.45, 129.34, 128.57, 128.54, 120.63, 116.48, 116.29, 116.11, 51.60, 51.15, 48.97, 48.59. HRMS (ESI) *m/z* for $C_{18}H_{18}FN_3OS$ $[M + H]^{--}$ calcd 344.1227, found 344.1224.

*4.1.1.15. 4-Methoxy-N-(4-phenylpiperazine-1-carbonothioyl)benzamide (**3o**).* White solid, yield 51 %, mp 135-137 ^{0}C. IR (KBr, cm^{-1}) 3433, 3269 (N-H str), 3039 (aromatic C-H str), 2933 (methyl C-H str), 1653 (amide C=O str), 1585 (N-H bend), 1526 (aromatic C=C str), 1449 (C-H sp^3 bend), 1285, 1210 (amine C-N str), 1029 (C-O str). ^{1}H NMR (500 MHz, $CDCl_3$) *δ*: 8.51 (s, 1H, NH), 7.85 (dd, *J* = 8.9, 1.9 Hz, 2H, Ar-H), 7.31 (dd, *J* = 8.7, 7.3 Hz, 2H, Ar-H), 7.01 – 6.92 (m, 5H, Ar-H), 4.40 (s, 2H, piperazine-H), 3.91 (s, 1H, piperazine-H), 3.90 (s, 3H, O-CH_3), 3.84 (s, 1H, piperazine-H), 3.39 (d, *J* = 34.2 Hz, 4H, piperazine-H). ^{13}C NMR (126 MHz, $CDCl_3$) *δ*: 182.54, 179.41, 165.92, 164.06, 163.55, 162.85, 150.37, 129.99, 129.87, 129.32, 124.48, 123.46, 120.53, 116.45, 114.45, 114.22, 55.59, 51.70, 51.24, 48.95, 48.61. HRMS (ESI) *m/z* for $C_{19}H_{21}N_3O_2S$ $[M + H]^+$ calcd 356.1427, found 356.1427.

*4.1.1.16. N-(diphenylcarbamothioyl)-4-methoxybenzamide (**3p**).* Fluorescent yellow solid, yield 54 %, mp 126-128 ^{0}C. IR (KBr, cm^{-1}) 3436, 3218 (N-H str), 3067 (aromatic C-H str), 2957 (methyl C-H str), 1688 (amide C=O str), 1587 (N-H bend), 1508 (aromatic C=C str), 1467 (C-H sp^3 bend), 1260 (amine C-N str), 1036 (C-O str). ^{1}H NMR (500 MHz, $CDCl_3$) *δ*: 8.69 (s, 1H, Ar-H), 8.04 (d, *J* = 8.9 Hz, 1H, Ar-H), 7.61 (d, *J* = 8.8 Hz, 2H, Ar-H), 7.32 – 7.24 (m, 4H, Ar-H), 7.10 (d, *J* = 8.3 Hz, 2H, Ar-H), 7.04 – 6.91 (m, 2H, Ar-H), 6.88 (d, *J* = 8.8 Hz, 2H, Ar-H), 3.92 (s, 1H, NH), 3.85 (s, 3H, O-CH_3). ^{13}C NMR (126 MHz, $CDCl_3$) *δ*: 182.80, 165.33, 163.31, 161.83, 160.82, 145.76, 143.13, 132.98, 129.80, 129.35, 127.38, 126.89, 124.87, 120.98, 117.80,

114.34, 114.04, 55.72, 55.50. HRMS (ESI) *m/z* for $C_{21}H_{18}N_2O_2S$ $[M + H]^{+}$ calcd 363.1162, found 363.1157.

*4.1.1.17. N-(diphenylcarbamothioyl)-4-nitrobenzamide (**3q**).* Light yellow solid, yield 42 %, mp 149-151 ^{0}C. IR (KBr, cm^{-1}) 3429, 3220 (N-H str), 3059 (aromatic C-H str), 1684 (amide C=O str), 1578 (N-H bend), 1542 (aromatic C=C str), 1515 (nitro N-O str), 1256 (amine C-N str). ^{1}H NMR (500 MHz, DMSO-d_6) δ: 11.57 (s, 1H, NH), 8.23 (d, J = 8.9 Hz, 2H, Ar-H), 7.84 (d, J = 8.9 Hz, 2H, Ar-H), 7.38 (t, J = 7.4 Hz, 4H, Ar-H), 7.31 (d, J = 7.6 Hz, 4H, Ar-H), 7.26 – 7.22 (m, 2H, Ar-H). ^{13}C NMR (126 MHz, DMSO-d_6) δ: 184.20, 162.33, 150.02, 143.89, 138.62, 131.17, 129.97, 129.65, 129.60, 127.71, 127.25, 124.24, 123.88, 120.10, 117.19. HRMS (ESI) *m/z* for $C_{20}H_{15}N_3O_3S$ $[M + H]^{+}$ calcd 378.0907, found 378.0903.

*4.1.2. General Procedure for the Synthesis of Compounds **2a-n**.* Benzoyl thiourea, **3a-q** (1 mmol) was treated with 2-bromoacetophenone (1 mmol) in the presence of base catalyst triethylamine in acetonitrile and reaction mixture was refluxed at 70 ^{0}C till completion of the reaction monitored with TLC (Scheme 2). Solvent was removed under reduced pressure. Crude solid obtained was washed with diethyl ether and recrystallized from ethanol/ethyl acetate to get pure products. Also pure product was eluted from column chromatography with hexane/ethyl acetate.

*4.1.2.1. Phenyl(4-phenyl-2-(piperidin-1-yl)thiazol-5-yl)methanone (**2a**).* Yellow solid, yield 70 %, mp 124-126 ^{0}C. IR (KBr, cm^{-1}) 3056, 3024 (aromatic C-H str), 1708 (C=O str), 1601 (C=N str), 1540 (aromatic C=C str), 1346 (thiazole C-N str), 1296, 1250 (aromatic amine C-N str), 720, 702 (C-S str). ^{1}H NMR (500 MHz, $CDCl_3$) δ: 7.46 (dd, J = 8.2, 1.2 Hz, 2H, Ar-H), 7.32 (dd, J = 8.1, 1.2 Hz, 2H, Ar-H), 7.24 (t, J = 7.4 Hz, 1H, Ar-H), 7.15 – 7.05 (m, 5H, Ar-H), 3.66 (s,

4H, piperidin-H), 1.73 (s, 6H, piperidin-H). ^{13}C NMR (126 MHz, $CDCl_3$) δ: 188.70, 171.78, 159.81, 138.59, 135.23, 131.06, 129.91, 129.10, 128.49, 127.54, 122.13, 49.32, 25.23, 23.98. HRMS (ESI) *m/z* for $C_{21}H_{20}N_2OS$ $[M + H]^+$ calcd 349.1369, found 349.1372.

*4.1.2.2. (2-Morpholino-4-phenylthiazol-5-yl)(phenyl)methanone (**2b**).* Yellow solid, yield 97 %, mp 126-128 ^{0}C. IR (KBr, cm^{-1}) 3041 (aromatic C-H str), 1710 (C=O str), 1600 (C=N str), 1534 (aromatic C=C str), 1347 (thiazole C-N str), 1291, 1264 (aromatic amine C-N str), 1112 (morpholine C-O-C), 723, 701 (C-S str). ^{1}H NMR (500 MHz, $CDCl_3$) δ: 7.48 (d, J = 7.7 Hz, 2H, Ar-H), 7.32 (d, *J* = 7.3 Hz, 2H, Ar-H), 7.26 (t, *J* = 7.4 Hz, 1H, Ar-H), 7.17 – 7.06 (m, 5H, Ar-H), 3.88 – 3.85 (m, 4H, morpholin-H), 3.69 – 3.66 (m, 4H, morpholin-H). ^{13}C NMR (126 MHz, $CDCl_3$) δ: 188.84, 171.87, 159.12, 138.16, 134.85, 131.40, 129.90, 129.17, 128.69, 127.65, 122.96, 66.10, 48.10. HRMS (ESI) *m/z* for $C_{20}H_{18}N_2O_2S$ $[M + H]^{--}$ calcd 351.1162, found 351.1158.

*4.1.2.3. Phenyl(4-phenyl-2-(pyrrolidin-1-yl)thiazol-5-yl)methanone (**2c**).* Light yellow solid, yield 57 %, mp 148-150 ^{0}C. IR (KBr, cm^{-1}) 3056 (aromatic C-H str), 1689 (C=O str), 1597 (C=N str), 1553 (aromatic C=C str), 1348 (thiazole C-N str), 1328, 1283 (aromatic amine C-N str), 713, 698 (C-S str). ^{1}H NMR (500 MHz, $CDCl_3$) δ: 7.43 (dd, *J* = 8.2, 1.2 Hz, 2H, Ar-H), 7.31 (dd, *J* = 8.2, 1.3 Hz, 2H, Ar-H), 7.22 (t, *J* = 7.5 Hz, 1H, Ar-H), 7.12 (t, *J* = 7.3 Hz, 1H, Ar-H), 7.07 (td, *J* = 7.5, 4.8 Hz, 4H, Ar-H), 3.61 (s, 4H, pyrrolidin-H), 2.14 – 2.09 (m, 4H, pyrrolidin-H). ^{13}C NMR (126 MHz, $CDCl_3$) δ: 188.73, 168.61, 160.30, 138.59, 135.25, 130.95, 129.94, 129.05, 128.47, 127.59, 127.51, 122.57, 49.73, 25.74. HRMS (ESI) *m/z* for $C_{20}H_{18}N_2OS$ $[M + H]^{--}$ calcd 335.1213, found 335.1173.

*4.1.2.4. (2-(Benzyl(methyl)amino)-4-phenylthiazol-5-yl)(phenyl)methanone (**2d**).* Yellow solid, yield 91 %, mp 126-127 ^{0}C. IR (KBr, cm^{-1}) 3052 (aromatic C-H str), 2915 (methyl C-H str), 2878 (CH_2 C-H str), 1823 (C=O str), 1604 (C=N str), 1551 (aromatic C=C str), 1475 (C-H sp^3 bend), 1331 (thiazole C-N str), 1285 (amine C-N str), 713, 700 (C-S str). ^{1}H NMR (500 MHz, $CDCl_3$) δ: 7.49 (d, J = 7.5 Hz, 2H, Ar-H), 7.42 – 7.34 (m, 7H, Ar-H), 7.26 (t, J = 7.4 Hz, 1H, Ar-H), 7.15 (t, J = 7.3 Hz, 1H, Ar-H), 7.10 (q, J = 7.9 Hz, 4H, Ar-H), 4.86 (s, 2H, N-CH_2), 3.17 (s, 3H, N-CH_3). ^{13}C NMR (126 MHz, $CDCl_3$) δ: 188.74, 171.97, 159.74, 138.47, 135.93, 135.11, 131.17, 130.01, 129.15, 128.85, 128.57, 127.95, 127.84, 127.57, 122.84, 56.14, 38.05. HRMS (ESI) *m/z* for $C_{24}H_{20}N_2OS$ $[M + H]^{+}$ calcd 385.1340, found 385.1340.

*4.1.2.5. (2-(Methyl(phenyl)amino)-4-phenylthiazol-5-yl)(phenyl)methanone (**2e**).* Brown solid, yield 89 %, mp 118-120 ^{0}C. IR (KBr, cm^{-1}) 3058 (aromatic C-H str), 2932 (methyl C-H str), 1689 (C=O str), 1635 (C=N str), 1594, 1579, 1512 (aromatic C=C str), 1469, 1403 (C-H sp^3 bend), 1310 (thiazole C-N str), 1284, 1265 (amine C-N str), 722, 697 (C-S str). ^{1}H NMR (500 MHz, $CDCl_3$) δ: 7.50 (dd, J = 20.8, 9.6 Hz, 6H, Ar-H), 7.38 (t, J = 7.7 Hz, 3H, Ar-H), 7.25 (t, J = 7.4 Hz, 1H, Ar-H), 7.16 (t, J = 7.2 Hz, 1H, Ar-H), 7.10 (dt, J = 10.4, 5.0 Hz, 4H, Ar-H), 3.69 (s, 3H, N-CH_3). ^{13}C NMR (126 MHz, $CDCl_3$) δ: 188.96, 171.44, 158.55, 145.35, 138.21, 134.79, 131.37, 130.20, 129.98, 129.18, 128.64, 127.82, 127.65, 125.49, 122.91, 40.41. HRMS (ESI) *m/z* for $C_{23}H_{18}N_2OS$ $[M + H]^{+}$ calcd 371.1213, found 371.1208.

*4.1.2.6. Phenyl(4-phenyl-2-(4-phenylpiperazin-1-yl)thiazol-5-yl)methanone (**2f**).* Light yellow solid, yield 94 %, mp 180-182 ^{0}C. IR (KBr, cm^{-1}) 3040 (aromatic C-H str), 1688 (C=O str), 1605 (C=N str), 1576, 1521,1497 (aromatic C=C str), 1338 (thiazole C-N str), 1269, 1210, 1162 (amine C-N str), 719, 698 (C-S str). ^{1}H NMR (500 MHz, $CDCl_3$) δ: 7.49 (d, J = 7.5 Hz, 2H, Ar-H), 7.34 (t, J = 7.4 Hz, 4H, Ar-H), 7.28 (d, J = 8.7 Hz, 1H, Ar-H), 7.18 – 7.08 (m, 5H, Ar-H),

7.01 (d, *J* = 8.1 Hz, 2H, Ar-H), 6.97 (t, *J* = 7.3 Hz, 1H, Ar-H), 3.89 – 3.83 (m, 4H, piperazine-H), 3.39 – 3.34 (m, 4H, piperazine-H). ^{13}C NMR (126 MHz, $CDCl_3$) *δ*: 188.83, 171.64, 159.40, 150.83, 138.26, 134.96, 131.34, 129.92, 129.35, 129.17, 128.66, 127.64, 122.98, 120.87, 116.96, 49.07, 47.99. HRMS (ESI) *m/z* for $C_{26}H_{23}N_3OS$ $[M + H]^{+}$ calcd 426.1635, found 426.1630.

*4.1.2.7. (2-(Diphenylamino)-4-phenylthiazol-5-yl)(phenyl)methanone (**2g**).* Light yellow solid, yield 95 %, mp 192-194 ^{0}C. IR (KBr, cm^{-1}) 3056 (aromatic C-H str), 1712 (C=O str), 1602 (C=N str), 1496, 1471, 1447 (aromatic C=C str), 1338 (thiazole C-N str), 1256, 1157 (amine C-N str), 720, 699 (C-S str). ^{1}H NMR (500 MHz, $CDCl_3$) *δ*: 7.56 – 7.49 (m, 6H, Ar-H), 7.46 (t, *J* = 7.8 Hz, 4H, Ar-H), 7.37 – 7.28 (m, 5H, Ar-H), 7.16 – 7.07 (m, 5H, Ar-H). ^{13}C NMR (126 MHz, $CDCl_3$) *δ*: 189.10, 170.58, 158.08, 144.21, 137.99, 134.70, 131.69, 130.00, 129.77, 129.31, 128.59, 127.73, 127.61, 126.88, 126.19, 124.32. HRMS (ESI) *m/z* for $C_{28}H_{20}N_2OS$ $[M + H]^{+}$ calcd 433.1369, found 433.1363.

*4.1.2.8. (4-(4-Methoxyphenyl)-2-(piperidin-1-yl)thiazol-5-yl)(phenyl)methanone (**2h**).* Yellow solid, yield 43 %, mp 122-124 ^{0}C. IR (KBr, cm^{-1}) 3056, 3004 (aromatic C-H str), 1680 (C=O str), 1590 (C=N str), 1529 (aromatic C=C str), 1346 (thiazole C-N str), 1292, 1249, 1163 (amine C-N str), 1025 (C-O str), 708 (C-S str). ^{1}H NMR (500 MHz, $CDCl_3$) *δ*: 7.50 (d, *J* = 8.8 Hz, 2H, Ar-H), 7.36 (dd, *J* = 8.2, 1.4 Hz, 2H, Ar-H), 7.13 (dt, *J* = 14.3, 7.0 Hz, 3H, Ar-H), 6.60 (d, *J* = 8.8 Hz, 2H, Ar-H), 3.75 (s, 3H, O-CH_3), 3.64 (s, 4H, piperidin-H), 1.72 (s, 6H, piperidin-H). ^{13}C NMR (126 MHz, $CDCl_3$) *δ*: 187.59, 171.50, 162.19, 158.64, 135.36, 131.51, 131.02, 129.91, 129.10, 128.41, 127.67, 121.88, 112.89, 55.31, 49.28, 25.22, 24.00. HRMS (ESI) *m/z* for $C_{22}H_{22}N_2O_2S$ $[M + H]^{+}$ calcd 379.1475, found 379.1470.

*4.1.2.9. (2-(Benzyl(methyl)amino)-4-(4-methoxyphenyl)thiazol-5-yl)(phenyl)methanone (**2i**).* Brown oil, yield 92 %. IR (KBr, cm^{-1}) 3060, 3028 (aromatic C-H str), 2930 (methyl C-H str), 2847 (CH_2 C-H str), 1681 (C=O str), 1599 (C=N str), 1544 (aromatic C=C str), 1474 (C-H sp^3 bend), 1327 (thiazole C-N str), 1252, 1172 (amine C-N str), 1028 (C-O str), 700 (C-S str). ^{1}H NMR (500 MHz, $CDCl_3$) δ: 7.51 (t, J = 8.1 Hz, 2H, Ar-H), 7.41 – 7.32 (m, 7H, Ar-H), 7.21 – 7.07 (m, 3H, Ar-H), 6.62 (d, J = 8.5 Hz, 2H, Ar-H), 4.85 (s, 2H, N-CH_2), 3.75 (d, J = 12.1 Hz, 3H, O-CH_3), 3.16 (s, 3H, N-CH_3). ^{13}C NMR (126 MHz, $CDCl_3$) δ: 187.56, 173.28, 171.59, 162.26, 135.27, 131.56, 131.48, 131.09, 130.93, 130.00, 129.15, 128.82, 128.47, 127.83, 127.67, 122.54, 113.05, 112.92, 55.32, 37.99, 25.37. HRMS (ESI) *m/z* for $C_{25}H_{22}N_2O_2S$ $[M + H]^{--}$ calcd 415.1475, found 415.1469.

*4.1.2.10. (4-(4-Nitrophenyl)-2-(4-phenylpiperazin-1-yl)thiazol-5-yl)(phenyl)methanone (**2j**).* Pale yellow solid, yield 57 %, mp 177-179 ^{0}C. IR (KBr, cm^{-1}) 3041 (aromatic C-H str), 1686 (C=O str), 1603 (C=N str), 1578, 1525 (aromatic C=C str), 1515 (nitro N-O str), 1336 (thiazole C-N str), 1266, 1211, 1161 (amine C-N str), 718, 699 (C-S str). ^{1}H NMR (500 MHz, $CDCl_3$) δ: 8.04 – 7.89 (m, 2H, Ar-H), 7.54 (dd, J = 13.0, 7.8 Hz, 3H, Ar-H), 7.36 – 6.96 (m, 9H, Ar-H), 3.87 (d, J = 18.9 Hz, 4H, piperazine-H), 3.37 (s, 4H, piperazine-H). ^{13}C NMR (126 MHz, $CDCl_3$) δ: 188.01, 172.27, 171.66, 164.45, 161.17, 156.14, 150.68, 148.69, 147.38, 141.28, 138.22, 132.11, 130.69, 129.91, 129.76, 129.37, 129.10, 128.74, 128.48, 128.03, 127.84, 122.77, 120.99, 117.00, 49.14, 48.11. HRMS (ESI) *m/z* for $C_{26}H_{22}N_4O_3S$ $[M + H]^+$ calcd 471.1485, found 471.1486.

*4.1.2.11. (4-(4-Fluorophenyl)-2-morpholinothiazol-5-yl)(phenyl)methanone (**2k**).* Yellow solid, yield 78 %, mp 124-126 ^{0}C. IR (KBr, cm^{-1}) 3043 (aromatic C-H str), 1712 (C=O str), 1602 (C=N str), 1538 (aromatic C=C str), 1346 (thiazole C-N str), 1290, 1258 (amine C-N str), 1116 (morpholine C-O-C), 1011 (C-F str), 720, 700 (C-S str). ^{1}H NMR (500 MHz, $CDCl_3$) δ: 7.48 (dd,

J = 7.9, 3.8 Hz, 2H, Ar-H), 7.35 – 7.27 (m, 3H, Ar-H), 7.18 – 7.09 (m, 2H, Ar-H), 6.77 (dd, *J* = 16.5, 8.6 Hz, 2H, Ar-H), 3.87 – 3.84 (m, 4H, morpholin-H), 3.67 (dd, *J* = 10.0, 5.1 Hz, 4H, morpholin-H). ^{13}C NMR (126 MHz, $CDCl_3$) *δ*: 188.63, 187.34, 171.84, 165.54, 163.91, 161.84, 159.12, 157.92, 138.17, 134.76, 134.30, 131.78, 131.72 , 131.55, 131.02, 129.87, 129.11, 128.81, 127.78, 122.73, 114.75, 114.57, 66.08, 48.08, 46.08. HRMS (ESI) *m/z* for $C_{20}H_{17}FN_2O_2S$ $[M + H]^+$ calcd 369.1068, found 369.1068.

*4.1.2.12. (4-(4-methoxyphenyl)-2-(4-phenylpiperazin-1-yl)thiazol-5-yl)(phenyl)methanone (**2l**).* Light yellow solid, yield 88 %, mp 140-142 ^{0}C. IR (KBr, cm^{-1}) 3045 (aromatic C-H str), 2988 (methyl C-H str), 1676 (C=O str), 1604 (C=N str), 1577, 1529 (aromatic C=C str), 1476 (C-H sp^3 bend), 1330 (thiazole C-N str), 1269, 1210, 1158 (amine C-N str), 1026 (C-O str), 698 (C-S str). ^{1}H NMR (500 MHz, $CDCl_3$) *δ*: 7.52 (t, *J* = 9.0 Hz, 2H, Ar-H), 7.41 – 7.31 (m, 4H, Ar-H), 7.15 (dt, *J* = 14.3, 7.0 Hz, 3H, Ar-H), 7.01 (d, *J* = 7.9 Hz, 2H, Ar-H), 6.96 (t, *J* = 7.3 Hz, 1H, Ar-H), 6.62 (d, *J* = 8.9 Hz, 2H, Ar-H), 3.86 – 3.82 (m, 4H, piperazine-H), 3.75 (d, *J* = 11.3 Hz, 3H, O-CH_3), 3.38 – 3.34 (m, 4H, piperazine-H). ^{13}C NMR (126 MHz, $CDCl_3$) *δ*: 188.78, 187.59, 171.30, 162.42, 160.04, 159.25, 158.10, 150.87, 135.12, 131.62, 131.40, 130.74, 129.90, 129.33, 129.17, 128.56, 127.76, 122.74, 120.82, 116.94, 113.14, 112.99, 55.34, 49.06, 47.99. HRMS (ESI) *m/z* for $C_{27}H_{25}N_3O_2S$ $[M + H]^{--}$ calcd 456.1740, found 456.1731.

*4.1.2.13. (2-(diphenylamino)-4-(4-methoxyphenyl)thiazol-5-yl)(phenyl)methanone (**2m**).* Fluorescent yellow solid, yield 70 %, mp 148-150 ^{0}C. IR (KBr, cm^{-1}) 3056 (aromatic C-H str), 2921 (methyl C-H str), 1670 (C=O str), 1596 (C=N str), 1492, 1470 (aromatic C=C str), 1446 (C-H sp^3 bend), 1332 (thiazole C-N str), 1252, 1156 (amine C-N str), 1026 (C-O str), 694 (C-S str). ^{1}H NMR (500 MHz, $CDCl_3$) *δ*: 7.58 (d, *J* = 8.9 Hz, 2H, Ar-H), 7.52 (dd, *J* = 8.6, 1.2 Hz, 4H, Ar-H), 7.48 – 7.38 (m, 6H, Ar-H), 7.31 (t, *J* = 7.4 Hz, 2H, Ar-H), 7.14 (dt, *J* = 14.3, 7.0 Hz, 3H,

Ar-H), 6.63 (dd, *J* = 12.5, 8.9 Hz, 2H, Ar-H), 3.75 (d, *J* = 16.8 Hz, 3H, O-CH_3). ^{13}C NMR (126 MHz, $CDCl_3$) *δ*: 187.77, 170.01, 162.71, 156.70, 144.32, 134.83, 131.80, 131.48, 130.52, 129.92, 129.73, 129.30, 128.48, 127.73, 126.72, 126.14, 124.05, 113.10, 55.35. HRMS (ESI) *m/z* for $C_{29}H_{22}N_2O_2S$ $[M + H]^{-}$ calcd 463.1475, found 463.1467.

*4.1.2.14. (2-(diphenylamino)-4-(4-nitrophenyl)thiazol-5-yl)(phenyl)methanone (**2n**).* Yellow solid, yield 70 %, mp 193-195 ^{0}C. IR (KBr, cm^{-1}) 3054 (aromatic C-H str), 1708 (C=O str), 1605 (C=N str), 1520 (nitro N-O str), 1494, 1470, 1444 (aromatic C=C str), 1338 (thiazole C-N str), 1257, 1154 (amine C-N str), 718, 697 (C-S str). ^{1}H NMR (500 MHz, $CDCl_3$) *δ*: 7.97 (d, *J* = 8.9 Hz, 2H, Ar-H), 7.56 (dd, *J* = 10.5, 8.0 Hz, 4H, Ar-H), 7.52 – 7.45 (m, 8H, Ar-H), 7.38 – 7.33 (m, 3H, Ar-H), 7.20 (t, *J* = 7.8 Hz, 2H, Ar-H). ^{13}C NMR (126 MHz, $CDCl_3$) *δ*: 188.27, 170.75, 154.95, 147.38, 143.92, 140.99, 137.91, 132.45, 130.67, 129.91, 129.24, 128.12, 127.22, 126.17, 125.37, 122.82. HRMS (ESI) *m/z* for $C_{28}H_{19}N_3O_3S$ $[M + H]^{-}$ calcd 478.1220, found 478.1213.

4.2. Biological studies and assays

Human recombinant 5-LOX-pT3 plasmid was received as a kind gift from Prof. Olof Rådmark, Karolinska Institute, Stockholm, Sweden. Luria–Bertani (LB) medium was purchased from BD, Biosciences, USA. Zileuton, 13(S) HpODE) and Arachidonic acid were obtained from Cayman Chemicals (Inalco, Milan, Italy). DPPH was procured from Sigma-Aldrich Chemie GmbH (Steinheim, Germany). All other fine chemicals and HPLC solvents were from Sigma-Aldrich (Steinheim, Germany), Merck (Mumbai, India), Sisco Research Laboratories, Spectrochem® and RANKEM®.

4.2.1. Expression and purification of 5-LOX

Human recombinant 5-LOX in a pT3 plasmid vector was transformed into *E. coli* BL21 bacteria and purification was performed as reported previously [43,44]. In brief, overnight grown bacterial culture in LB medium with 150 µg/mL ampicillin at 37 °C until OD_{600} reached above 0.5 was induced with 0.5 mM of isopropyl-D-thiogalactopyranoside (IPTG), followed by shaking overnight at 18 ^{o}C. Cells were pelleted out by centrifugation (Centrifuge 5804 R, Eppendorf AG) at 5000 rpm and 4 °C for 15 min and lysed by incubating in 50 mM of triethanolamine/HCl at a pH 8.0, 5 mM of ethylenediaminetetraacetic acid (EDTA), 60 µg/mL of trypsin inhibitor, 1 mM of phenylmethylsulphonylfluoride (PMSF) and 500 µg/mL of lysozyme. Further, cell lysate was homogenized by sonication for 42 s and centrifuged (Centrifuge 5418 R, Eppendorf AG) at 19000 × g and 4 °C for 15 min. Supernatant was precipitated with saturated ammonium sulfate (50 % w/v) during 45 min stirring on ice, centrifuged at 16000 × g and 4 °C for 30 min. The pellet was resuspended in Phosphate buffered saline (PBS) containing 1 mM EDTA and 1 mM PMSF and centrifuged at 100000 x g and 4 °C for 70 min. The supernatant collected was aliquoted and immediately used for 5-LOX activity assays.

4.2.2. 5-LOX inhibition assay in cell-free systems

For 5-LOX inhibition studies, an assay mixture containing 25 mM of HEPES, 2-[4-(2-hydroxyethyl)piperazin-1-yl]ethanesulfonic acid (pH 7.3), 0.4 M of ethylenediaminetetraacetic acid (EDTA), 10 mM of $CaCl_2$, 4 mM of adenosine 5'-triphosphate (ATP) was added to 5-LOX aliquot. Solutions of test compounds (10 µM) prepared in DMSO (2 % v/v) were mixed with the assay mixture at 4 °C [44]. The 5-LOX enzyme activity assay was started by the addition of the substrate AA at 30 µM. The activity was determined using UV absorbance at a λ_{max} of 236 nm

(Jasco V-550 UV–vis spectrophotometer) by measuring the product formation of 5(S)-hydroperoxy-6-trans-8,11,14-cis-eicosatetraenoic acid (5-HPETE) from AA. Zileuton was used as the positive control whose IC_{50} was found in agreement with the literature value [12]. IC_{50} values of other compounds were determined using GraphPad Prism version 5.01 from graph between percentage inhibition and various inhibitors concentrations. Each assay was repeated thrice and means ± SEM are given.

4.2.3. 5-LOX enzyme kinetic assay

The enzyme kinetics of human 5-LOX was studied for finding the mechanism of action of inhibitors. It was determined by measuring the formation of product, 5-HPETE at 236 nm in UV spectrophotometer in the same way as 5-LOX activity assay as described previously with modifications [45]. Substrate (AA) concentration was varied between 1–30 µM in the presence of three fixed concentrations (0, 5 and 10 µM) of inhibitor **2m** and **3f**. The rates of reactions which are change in concentration over time, were plotted against the substrate concentrations to determine K_m and V_{max} values. Lineweaver–Burk plot was plotted from the non-linear curve fitting data results. All the experiments were done in triplicates. Calculations were performed with GraphPad Prism 5.01.

4.2.4. Pseudoperoxidase activity assay

The pseudoperoxidase activity of 5-LOX determines the redox properties of inhibitors in the presence of 13-HPODE as oxidising product. The redox activity was monitered by the direct measurement of decrease in oxidising product in terms of UV absorbance at 234 nm (Jasco V-550 UV-Vis spectrophotometer). Reaction was initiated by the addition of 10 µM inhibitor (a 1:1

ratio to 13-HPODE) in buffer containing 50 mM potassium phosphate (pH 7.4), 0.3 mM $CaCl_2$, 0.1 mM EDTA, 200 μM ATP, 10 μM 13- (S)-HPODE. Zileuton, a known redox inhibitor was used as the positive control [35,46].

4.2.5. DPPH radical scavenging assay

The antioxidant activity of test compounds was evaluated using DPPH as described [39,47]. Briefly, test compounds at 20 μM were added to a solution of the stable free radical DPPH in methanol (0.1 mM) and incubated for 30 min at room temperature in dark. The absorbance was recorded in Multimode Plate reader (Enspire Perkin Elmer, version 4.10.3005.1440) at 517 nm and ascorbic acid was the reference molecule. Experiments were repeated thrice and data are given as mean ± SEM. The percentage of radical scavenging property was calculated using formula:

$$\% \text{ Inhibition} = \frac{(A_0 - A_s)}{A_0} \times 100$$

where, A_0 = absorbance of blank and A_s = absorbance of test sample.

4.2.6. Molecular docking

Molecular docking simulations were performed using Molecular operating environment (MOE; version 2016.0801, Chemical Computing Group, Suite 910, Canada) software. The X-ray crystal structure of human 5-LOX protein (PDB Code: 3O8Y) was taken from PDB. Protein preparation was done by removing all the heteroatoms such as water, non-receptor ions. Kollmann charges were assigned, hydrogens were added and energy was minimized AMBER99 force field.

Ligands were prepared by building their structures and minimizing their energies using MMFF94x force field in MOE. The key amino acids comprising of active site included: Trp147, Asn407, Thr364, His432, Phe421, Leu420, Phe177, Trp599, His600, Tyr181, Ala606, Leu373, His367, Leu414, Ile406, His550, Ile673 [48]. The selected ligands **2a**, **2b** and **2m** were then docked into the active site of the prepared protein. The binding energies of the top 100 poses were calculated using LondondG as 1st and GBVI/WSAdG as 2nd rescoring methodologies. The docking poses with H-bonds and low binding free energies were used for analyzing ligand-receptor interaction and considered as the best fit for the protein.

4.2.7. Pharmacophore elucidation

The pharmacophore modeling of essential features required for the biological activity was performed in MOE; version 2016.0801, Chemical Computing Group, Quebec, Canada using 'Pharmacophore elucidation'. Chemical structures were built, energy minimized and pharmacophore conformational library has been developed. Pharmacophore elucidation and search are done on pharmacophore editor in MOE workstation for the query of hit molecules [49]. The data is viewed in database viewer and saved in .ph4 format.

Acknowledgements

S. S acknowledges DST, New Delhi, WOS-A (SR/WOS-A/CS-126/2013), GoI for financial support and fellowship. The authors thank SAIF, IIT-Madras for NMR and IR spectral analysis and department of biotechnology, IIT-Madras for HRMS analysis.

Abbreviations

AA, Arachidonic acid; DMF, N,N-dimethylformamide; DMSO, Dimethyl sulphoxide; DPPH, 2,2 -diphenyl-1-picrylhydrazyl; EDTA, Ethylenediaminetetra acetic acid; 5-HPETE, 5(S) hydroperoxyeicosatetraenoic acid; 13(S) HpODE, 13(S)-hydroperoxyoctadecadienoic acid; 5-LOX, 5-Lipoxygenase; LB, Lineweaver–Burk; LT, Leukotriene; Ph, Pharmacophore; PMSF, Phenylmethyl sulphonyl fluoride; TMS, Tetramethylsilane.

References

1. D.A. Medina-Tato, M.L. Watson, S.G. Ward, Leukocyte navigation mechanisms as targets in airway diseases, Drug Discovery Today, 11 (2006) 866-879.
2. L.M. Coussens, Z. Werb, Inflammation and cancer, Nature, 420 (2002) 860-867.
3. J.Z. Haeggström, A. Rinaldo-Matthis, C.E. Wheelock, A. Wetterholm, Advances in eicosanoid research, novel therapeutic implications, Biochemical and Biophysical Research Communications, 396 (2010) 135-139.
4. W.L. Smith, R.C. Murphy, The eicosanoids: cyclooxygenase, lipoxygenase, and epoxygenase pathways, New Comprehensive Biochemistry, 36 (2002) 341-371.
5. E. Ricciotti, G.A. FitzGerald, Prostaglandins and inflammation, Arteriosclerosis, Thrombosis, and Vascular Biology, 31 (2011) 986-1000.
6. O. Rådmark, Arachidonate 5-lipoxygenase, Prostaglandins & Other Lipid Mediators, 68 (2002) 211-234.
7. O. Rådmark, B. Samuelsson, Regulation of the activity of 5-lipoxygenase, a key enzyme in leukotriene biosynthesis, Biochemical and Biophysical Research Communications, 396 (2010) 105-110.
8. C. Pergola, O. Werz, 5-Lipoxygenase inhibitors: a review of recent developments and patents, Expert opinion on therapeutic patents, 20 (2010) 355-375.

9. R. Filosa, A. Peduto, A.M. Schaible, V. Krauth, C. Weinigel, D. Barz, C. Petronzi, F. Bruno, F. Roviezzo, G. Spaziano, Novel series of benzoquinones with high potency against 5-lipoxygenase in human polymorphonuclear leukocytes, European Journal of Medicinal Chemistry, 94 (2015) 132-139.
10. M. Gaba, C. Mohan, Design, Synthesis and Biological Evaluation of Novel 1, 2, 5-Substituted Benzimidazole Derivatives as Gastropro-tective Anti-inflammatory and Analgesic Agents, Med Chem, 5 (2015) 058-063.
11. D. De Lucia, O.M. Lucio, B. Musio, A. Bender, M. Listing, S. Dennhardt, A. Koeberle, U. Garscha, R. Rizzo, S. Manfredini, Design, synthesis and evaluation of semi-synthetic triazole-containing caffeic acid analogues as 5-lipoxygenase inhibitors, European Journal of Medicinal Chemistry, 101 (2015) 573-583.
12. G.W. Carter, P.R. Young, D.H. Albert, J. Bouska, R. Dyer, R.L. Bell, J.B. Summers, D. Brooks, 5-lipoxygenase inhibitory activity of zileuton, Journal of Pharmacology and Experimental Therapeutics, 256 (1991) 929-937.
13. S.P. Khanapure, D.S. Garvey, D.R. Janero, L. Gordon Letts, Eicosanoids in inflammation: biosynthesis, pharmacology, and therapeutic frontiers, Current Topics in Medicinal Chemistry, 7 (2007) 311-340.
14. N.S. Devi, M. Ramanan, P. Paragi-Vedanthi, M. Doble, Phytochemicals as multi-target inhibitors of the inflammatory pathway-A modeling and experimental study, Biochemical and Biophysical Research Communications, 484 (2017) 467-473.
15. M. T Chhabria, S. Patel, P. Modi, P. S Brahmkshatriya, Thiazole: a review on chemistry, synthesis and therapeutic importance of its derivatives, Current Topics in Medicinal Chemistry, 16 (2016) 2841-2862.
16. R.N. Sharma, F.P. Xavier, K.K. Vasu, S.C. Chaturvedi, S.S. Pancholi, Synthesis of 4-benzyl-1, 3-thiazole derivatives as potential anti-inflammatory agents: an analogue-based drug design approach, Journal of Enzyme Inhibition and Medicinal Chemistry, 24 (2009) 890-897.

17. F.W. Bell, A.S. Cantrell, M. Hoegberg, S.R. Jaskunas, N.G. Johansson, C.L. Jordan, M.D. Kinnick, P. Lind, J.M. Morin Jr, Phenethylthiazolethiourea (PETT) compounds, a new class of HIV-1 reverse transcriptase inhibitors. 1. Synthesis and basic structure-activity relationship studies of PETT analogs, Journal of Medicinal Chemistry, 38 (1995) 4929-4936.
18. C.B. Rödl, D. Vogt, S.B. Kretschmer, K. Ihlefeld, S. Barzen, A. Brüggerhoff, J. Achenbach, E. Proschak, D. Steinhilber, H. Stark, Multi-dimensional target profiling of N, 4-diaryl-1, 3-thiazole-2-amines as potent inhibitors of eicosanoid metabolism, European Journal of Medicinal Chemistry, 84 (2014) 302-311.
19. T. Hanke, F. Dehm, S. Liening, S.-D. Popella, J. Maczewsky, M. Pillong, J. Kunze, C. Weinigel, D. Barz, A. Kaiser, Aminothiazole-featured pirinixic acid derivatives as dual 5-lipoxygenase and microsomal prostaglandin E2 synthase-1 inhibitors with improved potency and efficiency in vivo, Journal of Medicinal Chemistry, 56 (2013) 9031-9044.
20. S. Sinha, T. Sravanthi, S. Yuvaraj, S. Manju, M. Doble, 2-Amino-4-aryl thiazole: a promising scaffold identified as a potent 5-LOX inhibitor, RSC Advances, 6 (2016) 19271-19279.
21. https://www.thepharmaletter.com/article/millennium-drops-oral-formulation-of-asthma-drug-mln977.
22. J. Malec, W. Przybyszewski, M. Grabarczyk, E. Sitarska, Hydroxyurea has the capacity to induce damage to human erythrocytes which can be modified by radical scavengers, Biochemical and Biophysical Research Communications, 120 (1984) 566-573.
23. D.A. Smith, A. Harrison, P. Morgan, Multiple factors govern the association between pharmacology and toxicity in a class of drugs: toward a unification of class effect terminology, Chemical research in toxicology, 24 (2011) 463-474.
24. Y. Wu, C. He, Y. Gao, S. He, Y. Liu, L. Lai, Dynamic modeling of human 5-lipoxygenase–inhibitor interactions helps to discover novel inhibitors, Journal of medicinal chemistry, 55 (2012) 2597-2605.

25. P. Aparoy, K.K. Reddy, S.K. Kalangi, T.C. Reddy, P. Reddanna, Pharmacophore modeling and virtual screening for designing potential 5-Lipoxygenase inhibitors, Bioorganic & Medicinal Chemistry Letters, 20 (2010) 1013-1018.

26. J.L. Masferrer, B.S. Zweifel, M. Hardy, G.D. Anderson, D. Dufield, L. Cortes-Burgos, R.A. Pufahl, M. Graneto, Pharmacology of PF-4191834, a novel, selective non-redox 5-lipoxygenase inhibitor effective in inflammation and pain, Journal of Pharmacology and Experimental Therapeutics, 334 (2010) 294-301.

27. D. Steinhilber, B. Hofmann, Recent Advances in the Search for Novel 5-Lipoxygenase Inhibitors, Basic & clinical pharmacology & toxicology, 114 (2014) 70-77.

28. S.L. Manju, S. Asha, T.F. Reji, K.N. Rajasekharan, Synthesis of novel substituted 4, 4'-(1, 4-phenylene) bis (1, 3-thiazole) s, ARKIVOC, (2008) 288-296.

29. D.N. Darji, T. Pasha, A. Bhandari, K. Molvi, S.A. Desai, M.V. Makwana, Synthesis of some novel 2, 4, 5–trisubstituted thiazoles as possible antibacterial agents, J. Chem. Pharm. Res, 4 (2012) 2148-2152.

30. R. Wisastra, P.A. Kok, N. Eleftheriadis, M.P. Baumgartner, C.J. Camacho, H.J. Haisma, F.J. Dekker, Discovery of a novel activator of 5-lipoxygenase from an anacardic acid derived compound collection, Bioorganic & Medicinal Chemistry, 21 (2013) 7763-7778.

31. O. Werz, D. Steinhilber, Development of 5-lipoxygenase inhibitors—lessons from cellular enzyme regulation, Biochemical pharmacology, 70 (2005) 327-333.

32. H. Lineweaver, D. Burk, The determination of enzyme dissociation constants, Journal of the American chemical society, 56 (1934) 658-666.

33. R.N. Young, Inhibitors of 5-lipoxygenase: a therapeutic potential yet to be fully realized?, European Journal of Medicinal Chemistry, 34 (1999) 671-685.

34. M.G. Chini, R. De Simone, I. Bruno, R. Riccio, F. Dehm, C. Weinigel, D. Barz, O. Werz, G. Bifulco, Design and synthesis of a second series of triazole-based compounds as potent dual

mPGES-1 and 5-lipoxygenase inhibitors, European Journal of Medicinal Chemistry, 54 (2012) 311-323.

35. J.-P. Falgueyret, J.H. Hutchinson, D. Riendeau, Criteria for the identification of non-redox inhibitors of 5-lipoxygenase, Biochemical Pharmacology, 45 (1993) 978-981.
36. S. Lee, Y. Park, J. Kim, S.-J. Han, A fluorescence-based assay for measuring the redox potential of 5-lipoxygenase inhibitors, PloS One, 9 (2014) e87708.
37. B.S. Zweifel, M.M. Hardy, G.D. Anderson, D.R. Dufield, R.A. Pufahl, J.L. Masferrer, A rat air pouch model for evaluating the efficacy and selectivity of 5-lipoxygenase inhibitors, European Journal of Pharmacology, 584 (2008) 166-174.
38. C. Kemal, P. Louis-Flamberg, R. Krupinski-Olsen, A.L. Shorter, Reductive inactivation of soybean lipoxygenase 1 by catechols: a possible mechanism for regulation of lipoxygenase activity, Biochemistry, 26 (1987) 7064-7072.
39. P. Sivakumar, P. Prabhakar, M. Doble, Synthesis, antioxidant evaluation, and quantitative structure–activity relationship studies of chalcones, Medicinal Chemistry Research, 20 (2011) 482-492.
40. J.B. Baell, G.A. Holloway, New substructure filters for removal of pan assay interference compounds (PAINS) from screening libraries and for their exclusion in bioassays, Journal of Medicinal Chemistry, 53 (2010) 2719-2740.
41. J.B. Baell, L. Ferrins, H. Falk, G. Nikolakopoulos, PAINS: Relevance to tool compound discovery and fragment-based screening, Australian Journal of Chemistry, 66 (2014) 1483-1494.
42. J. Baell, M.A. Walters, Chemical con artists foil drug discovery, Nature, 513 (2014) 481.
43. Y.Y. Zhang, O. Rådmark, B. Samuelsson, Mutagenesis of some conserved residues in human 5-lipoxygenase: effects on enzyme activity, Proceedings of the National Academy of Sciences, 89 (1992) 485-489.

44. L. Fischer, D. Szellas, O. Rådmark, D. Steinhilber, O. Werz, Phosphorylation-and stimulus-dependent inhibition of cellular 5-lipoxygenase activity by nonredox-type inhibitors, The FASEB Journal, 17 (2003) 949-951.

45. D. Ribeiro, M. Freitas, S.M. Tomé, A.M. Silva, G. Porto, E.J. Cabrita, M.M.B. Marques, E. Fernandes, Inhibition of LOX by flavonoids: a structure–activity relationship study, European journal of medicinal chemistry, 72 (2014) 137-145.

46. E.K. Hoobler, G. Rai, A.G. Warrilow, S.C. Perry, C.J. Smyrniotis, A. Jadhav, A. Simeonov, J.E. Parker, D.E. Kelly, D.J. Maloney, Discovery of a novel dual fungal CYP51/human 5-lipoxygenase inhibitor: implications for anti-fungal therapy, PloS One, 8 (2013) e65928.

47. C. Greiner, C. Hörnig, A. Rossi, C. Pergola, H. Zettl, M. Schubert-Zsilavecz, D. Steinhilber, L. Sautebin, O. Werz, 2-(4-(Biphenyl-4-ylamino)-6-chloropyrimidin-2-ylthio) octanoic acid (HZ52)–a novel type of 5-lipoxygenase inhibitor with favourable molecular pharmacology and efficacy in vivo, British Journal of Pharmacology, 164 (2011) 781-793.

48. N.C. Gilbert, S.G. Bartlett, M.T. Waight, D.B. Neau, W.E. Boeglin, A.R. Brash, M.E. Newcomer, The structure of human 5-lipoxygenase, Science, 331 (2011) 217-219.

49. P. Aparoy, K.K. Reddy, S.K. Kalangi, T.C. Reddy, P. Reddanna, Pharmacophore modeling and virtual screening for designing potential 5-Lipoxygenase inhibitors, Bioorganic & Medicinal Chemistry Letters, 20 (2010) 1013-1018.